Volume 12(3)
3rd Quarter 1997

ISSN: 0127-7065

JOURNAL OF NATURAL RUBBER RESEARCH

Price

Malaysia:	*RM30 per Issue* *RM100 per Volume*
Other countries:	*US$15 per Issue* *US$50 per Volume*

JOURNAL OF NATURAL RUBBER RESEARCH

EDITORIAL BOARD

EDITORIAL COMMITTEE

Rubber Research Institute of Malaysia (RRIM)
Malaysian Rubber Research and Development Board (MRRDB)
Tun Abdul Razak Research Centre (TARRC)

First published as the *Journal of the Rubber Research Institute of Malaya* in 1929.
Each volume of the *Journal of Natural Rubber Research* constitutes four issues published quarterly in March, June, September and December each year.

Published by the Rubber Research Institute of Malaysia
Printed by Cetaktama Sdn. Bhd.
1997

Contents

J. nat. Rubb. Res.
Volume 12(3), 1997

J. nat. Rubb. Res., **12(3)**, 131–141

Crack Growth and Strain Induced Anisotropy in Carbon Black Filled Natural Rubber †

J.J.C. BUSFIELD*#, C.H. RATSIMBA* AND A.G. THOMAS*

The work discussed outlines the development of a technique to predict failure of rubber components under repeated complex stressing. A fracture mechanics approach is adopted, which has been shown to work with simple plane stress type geometry in the past. Real components with three dimensional loading and geometry can be examined with the use of finite element analysis techniques. These now allow us to investigate real fracture type problems to large strain deformations.

To predict fatigue behaviour in components it is necessary to derive the energy release rate for that particular component, which in general involves FEA techniques. Also it is important to know the crack growth characteristics of the material. This is usually expressed in terms of the rate of crack growth as a function of the tearing energy (energy release rate). Conventional tearing energy, crack growth rate tests are performed in relatively simple deformation modes, using for example edge crack or pure shear test pieces. In practice, components used in engineering undergo more complicated strain histories. In order to study these potential complexities in the crack growth characteristics, the effect of pre-strain on cyclic crack growth behaviour using a predominantly pure shear test piece with an applied pre-strain has been studied. For the filled compounds studied so far there do appear to be complications and the observed crack growth rates may be substantially increased by these pre-strains. Some of these results are presented and their consequences discussed.

Catastrophic tearing studies[1,2] show that highly pre-stretched rubber sheets, are significantly weaker in the direction of pre-straining than in the direction running at a right angle to it. This strain induced anisotropy is shown most clearly in materials such as natural rubber that crystallise on straining. It is also much more obvious for typical engineering compounds filled with reinforcing carbon blacks.

Indeed carbon-black filled natural rubber compounds show a pre-strain induced anisotropy in strength even after the removal of the prior extension[1].

These differences in strength in different directions, induced either by a previous deformation or by the present one are of considerable interest. They may be responsible for the phenomenon known as knotty tearing, when the advancing crack profile spontaneously deviates from the anticipated path which is at right angles to the principle tensile stress field and turns instead in the direction of the stressed

---

† Paper presented at the International Rubber Conference 1997 Malaysia, 6–9 October, Kuala Lumpur

* Materials Department Queen Mary & Westfield College, University of London, London E1 4NS, United Kingdom

Corresponding author

direction. This causes an effective blunting of the crack tip and arrests the crack growth until the applied stress exceeds a new threshold value. This 'stick slip' behaviour is a characteristic of filled materials and appears to be one of the principle mechanisms of carbon black reinforcement.

This change of strength properties caused by a pre-straining has many practical applications, for example in predicting the failure behaviour of tyres or other inflated devices. This is even the case with more general engineering components such as those encountered in suspension systems, when a complex loading is encountered. Measures of strength taken from uni-axial deformations are likely therefore to be misleading.

In order to formulate a more scientific approach, the derivation of a fundamental measure of strength is necessary. The approach adopted most commonly is due originally to Griffith[3]. This leads to the assumption that the elastic energy available to drive a crack, T, determines the rate of crack growth. Where the tearing energy, T, may be defined as:

$$T = -\left(\frac{\partial U}{\partial A}\right)_v \qquad \ldots 1$$

U is the total strain energy stored in a specimen containing a crack and A the area of one of the cracks fracture surfaces. The differentiation is done over a constant deformation so that the external forces do not work.

Rapid crack growth tearing in specimens loaded or strained at a continuous rate usually utilise the trouser test. Many rubber components experience repeated cyclic loading in service sometimes causing cyclic crack growth to occur at much slower rates than those normally associated with the catastrophic single cycle tear test.

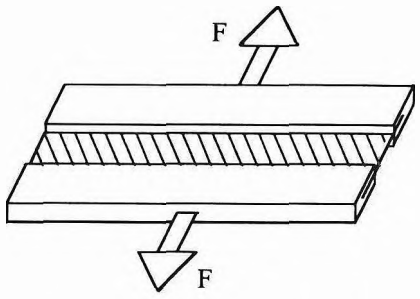

Figure 1. Pure shear test piece.

Cyclic crack growth tests can be investigated using a variety of different sample test geometries such as: the trouser test piece; the pure shear test piece shown schematically in *Figure 1*, and the edge cut tensile strip. Of these, the edge cut tensile strip tests result in continuously increasing crack growth rate per cycle while the pure shear geometry test results in constant crack growth per cycle, for a specified applied stress or a given tearing energy. The pure shear test piece will be used throughout our study, because of this effect.

The applicability of this approach has been verified by a number of researchers[4–6] using various test pieces cut from thin rubber sheets. This approach shows that a crack growth rate, dc/dN, *versus* tearing energy, T, relationship exists that is normally shown on a double logarithmic plot. Here, c is the crack length and, N, the number of cycles completed. This relationship is a basic material property that is independent of the test piece geometry for uni-axial load cases. Failure under repeated stressing appears to be initiated from small

naturally occurring defects or flaws in the object. The exact nature of these flaws is often unclear, however filler agglomerates or dirt particles are probably two of the major contributors.

In order to use the fracture mechanics approach the size, shape and orientation of the flaw relative to the applied stress field must be taken into account. Most rubber components have to be considered as three dimensional, and in order to calculate energy release rates large strain finite element techniques are required. Finite element techniques[7–9] have been used before to derive solutions to fracture problems at large strains in elastomers. However the application of this methodology to predict crack growth behaviour in real components has been slow to be realised.

Steady state crack growth behaviour measured in cyclical deformations on filled elastomers, for example as shown by De[10], also show rough fracture surfaces. The roughness of these fracture surfaces are much smaller in scale than that observed from knotty tearing using the trouser tear test piece, and obviously the associated tearing energies are much smaller.

However the roughness may still be associated with small scale anisotropy, developed in the direction of the strain, normal to the direction of the crack growth. If this is the case then an applied pre-strain in the direction of the crack growth should reduce the effect and may, if the pre-strain is sufficiently large, produce an anisotropy in the crack growth direction, resulting in reduced tearing energies.

In order to investigate and understand this strain induced anisotropy phenomenon, a series of tests have been conducted on three natural rubbers of varying carbon black content.

In the pure shear test, the width of the specimen is much greater than the height (finite element studies have shown that this should be at least 8 times). When the clamps are pulled apart, the test piece undergoes a pure shear deformation because the clamps effectively prevent the rubber strip from decreasing in width.

The first experiment is designed to investigate the deviation of the stress *versus* strain behaviour of a normal isotropic material caused by different levels of perpendicular pre-straining. Secondly, measurements are made of the cyclic crack growth behaviour at various levels of pre-strain and tearing energy and finally, an investigation is made into the effect of an applied and then removed pre-strain on the cyclic crack growth behaviour.

It has been shown by Davies *et al.*[11] that the stress strain behaviour of a carbon black filled natural rubber material can be expressed in terms of a single stored energy function over a wide range of strains and deformations, even when that stored energy function is a term of the first strain invariant, I_1 only. Where:

$$I_1 = \lambda_1^2 + \lambda_2^2 + \lambda_3^2 \qquad ...2$$

It should be possible therefore to measure and fit the stress *versus* strain data, measured by a tensile test, and derive the functional relationship to the proposed stored energy function. This stored energy function could then be used to predict the behaviour of a more complex pre-strained pure shear test piece and comparison could be made with experimental results.

The Davies *et al.* function is designed to predict the behaviour of engineering materials from small strains to reasonable strains of about 200%. As the current experiments do not measure the behaviour accurately at the small strains, it is possible to adopt a simpler stored energy function, involving only a power series in I_1. For example the function proposed by Yeoh[12]:

$$W = A_1(I_1 - 3) + A_2(I_1 - 3)^2 + A_3(I_1 - 3)^3 \quad ...3$$

Rivlin[13] has showed that the general relationship for the engineering stress σ_2 measured in the perpendicular direction as the grips are pulled apart, for the bi-axial deformation mode is given by:

$$\frac{\sigma_2 \lambda_2}{\lambda_2^2 - \left[\frac{1}{\lambda_1 \lambda_2}\right]^2} = 2\left[\frac{\partial W}{\partial I_1}\right] \quad ...4$$

where,

$$I_1 = \left[\lambda_1^2 + \lambda_2^2 + \frac{1}{(\lambda_1 \lambda_2)^2}\right] \quad ...5$$

Figure 2 shows a pure shear test piece containing a cut of length, c, and having an un-strained height, L_0, and thickness, t. Initially ignoring the effects of the pre-strain, if the specimen grips are held at a constant displacement to produce a strain λ_2, the strain energy density of the deformed pure shear specimen is not the same in all the different regions illustrated. Region A is unstressed and so the assumed strain energy U_A will be zero. In region B, around the cut tip, the stress field is complex and the strain energy U_B is difficult to determine. Region D will be in pure shear and so the strain energy function in this region will be given by $U_D = W V_D$ where W is the strain energy per unit volume of the material in pure shear at a specified strain and V_D is the volume of region D. The region E is in a more complex state of stress because of the edge effects.

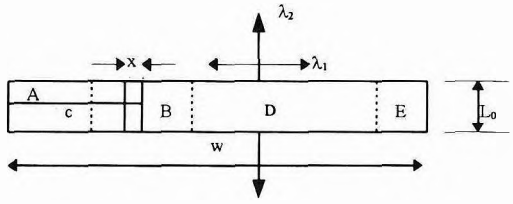

Figure 2. A schematic of the various stresses regions in a pre-strained test pure shear test piece, with a cut of length, c. The undeformed dimensions are defined.

When the crack length increases by dc, a simple transfer of material from region D to region A takes place and the total reduction in the stored energy is:

$$dU = W L_0 \, dc \quad ...6$$

where W is the strain energy density in pure shear and L_0 is the initial height of the specimen.

This leads to a simple expression for the tearing energy of:

$$T = W L_0 \quad ...7$$

However due to a cyclical stress softening effects, it is not easy to use this relationship to calculate the reduction in the tearing energy caused by the advancing crack. Therefore an alternative expression of the tearing energy is used in our calculations. By defining U the elastic stored energy which is equal to the area under the force-deflection curve and V the volume of the specimen contributing to the force-deflection curve, then $W = U/V$. By imposing an incompressible material constraint, the expression of V as referred to the un-strained dimensions is:

$$V = L_0\, t(w-c) \qquad \ldots 8$$

where L_0 is the un-strained height, t is the thickness, w the width and c the crack length. This expression assumes that only the volume of the uncut specimen contributes to the force-deflection curve and the cut part of the specimen is totally zero energy; which is untrue. Finite element studies indicate that an equivalent strip of width, x, of the cut specimen is not free of energy, where x had been determined by the analysis to be equal to 14% of L_0. Therefore a suitable expression for T is:

$$T = \frac{U}{t(w - c + x)} \qquad \ldots 9$$

For the pre-strained case where the test piece is pulled to a strain of λ_1 in the orthogonal direction prior to being clamped in the test grips, this tearing energy relationship has to be modified. For definition purposes all the dimensions referred to in the pre-strained state are indicated by a prime sign, therefore; t' for the thickness, c' the crack length, L_0' the height and w' the width.

When the crack propagates a length of $\Delta c'$, only regions A and D have a change in their elastic energy. If W_A and W_D are the strain energy densities, respectively in regions A and D, then the tearing energy for the system can be shown to be given by:

$$T = L_0\,(W_D - W_A) \qquad \ldots 10$$

As is known for the conventional pure shear test, L_0 is difficult to determine because of the stress-softening effects. Therefore another expression for deriving the tearing energy relationship is required.

Ignoring edge effects, $W_D - W_A$, which is now defined as the area under the force-deflection curve, U_S, divided by the volume of the specimen contributing to the force-deflection curve. This is the volume of the uncut specimen corrected by a term x'. This indicates that a vertical strip of width x' of the cut specimen contributes to the force-deflection curve:

$$V = L_0' t'(w' - c' + x') \qquad \ldots 11$$

From a finite element analysis of a specimen pre-strained 100% the value for x is calculated as being 19% of the un-strained height L_0. Therefore we can assume that:

$$x' = \lambda_1 x = \lambda_1 0.19 L_0 \qquad \ldots 12$$

This assumption that the original strip of width x will increase by a factor of λ_1 if a pre-strain λ_1 is applied has also been verified analytically by using finite element analysis. We finally obtain:

$$T = \frac{U_s \sqrt{\lambda_1}}{t'(w' - c' + x')} = \frac{U_s \lambda_1}{t(w' - c' + x')} \quad \ldots 13$$

In tearing tests it has been observed that a prior pre-strain in the direction of the crack propagation causes a weakening of the material when an orthogonal tear test is performed. This suggests that some form of permanent damage or orientation has taken place. In order to investigate this phenomenon further it is proposed to conduct cyclic crack growth tests on our materials after the pre-strain is removed and compare the results with materials tested from a virgin state.

EXPERIMENTS

The three materials used are summarised in *Table 1*.

All the testing was performed using the pure shear test piece geometry. The pre-straining was achieved by performing a simple tensile test on a strip of rubber until the desired pre-strain extension was reached. The rubber was then gripped, *in situ*, along its free edges by the pure shear grips. It was then removed from the tensile test machine. The pre-strain application remained because of the shape induced constraints of the test piece geometry. From this test piece the stress strain behaviour can again be measured using an Instron test machine.

Cyclic crack growth tests were carried out using a servo-hydraulic testing machine operating at room temperature. A sinusoidal wave function of the correct displacement at a frequency of 5 Hz was imposed on the specimen. The pure shear test-piece was strained to a maximum strain amplitude of between 5%–35% and relaxed to zero strain in each cycle.

TABLE 1. COMPOUNDS USED IN THE INVESTIGATION

Material	HAF N330 Carbon Black content (parts per hundred rubber)
A	21
B	32
C	50

All the materials use typical semi-EV curing systems. The square flat sheets (175 mm × 175 mm) were all cured for 10 min at 155°C

A horizontal cut of 40 mm in length was introduced on the central axis of one edge of the test piece using a razor blade. This placed the crack/cut tip sufficiently far from the edge to avoid any edge effects.

The crack length was measured using a magnifying, time lapse video camera and recorder, and load-displacement curves were simultaneously recorded to measure the tearing energy.

Due to the initial sharp crack tip the crack grows rapidly; however, as the crack grows the normal blunting of the crack tip occurs and the behaviour becomes more typical of steady state behaviour. It is after this initial time that crack growth rates were measured.

The pre-strained test pieces were easy to prepare, a rubber strip that was 175 mm long was pulled to the required single pre-strain for five minutes. It was then relaxed for 2 h to allow the dimensions to stabilise. The sheet is then tested under the conventional cyclical conditions.

RESULTS AND DISCUSSION

The curve fitting parameters for the stored energy function and predicted stress strain behaviour which are derived from simple tensile tests on the three materials, are tabulated in *Table 2.*

TABLE 2. CURVE FITTING PARAMETERS FOR THE STORED ENERGY FUNCTION SHOWN IN *EQUATION 3*

Material	A1/MPa	A2/MPa	A3/MPa
A	0.2630	–0.0006	0.0004
B	0.4629	–0.0009	0.0029
C	0.9643	–0.0013	0.0142

These parameters are all derived from tensile tests

Figure 3 shows a sample of the typical results displaying the agreement between the measured pre-strained results and those predicted if the material was exhibiting perfectly elastic isotropic behaviour.

In general for material B at the 50% pre-strains the predictions up to extensions of 100% are quite good. For higher pre-strains, the experimental data lies somewhat above the predictions. For the more highly filled material at a rather lower pre-strain, this is also the case.

This may be accounted for by the recovery of the black structure that may have broken down during the pre-straining process. This leads to a corresponding increase in the stiffness that can not be accounted for by the use of a stored energy function that assumes perfect elasticity.

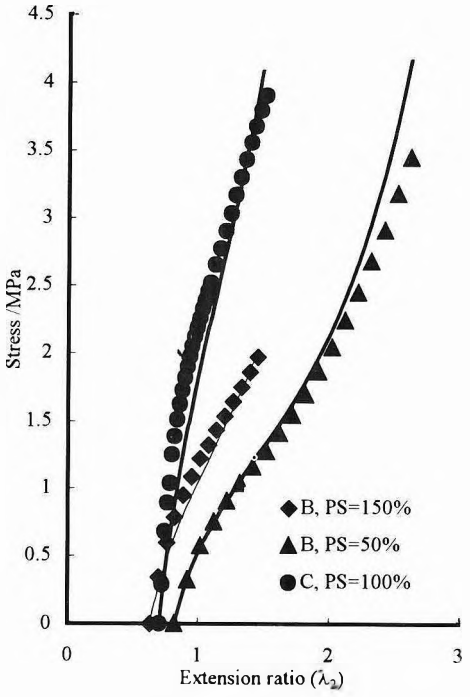

Figure 3. Three typical sets of data curves are shown for material B at both 50% and 150% pre-strains and material C at 100% pre-strain. The points represent the measured data and the lines represent the prediction from the theoretial relationship.

Figures 4, 5 and *6* show the tearing energy *versus* crack growth relationships for three materials.

At the lower tearing energies, the effect of pre-strain is broadly similar. A pre-strain of 100% reduces the T value for the material A and B by a factor of 3.5 and for material C by a factor of 8.5.

For the highly filled compound C, at the higher tearing energies and at high pre-strains the crack growth rate increases dramatically.

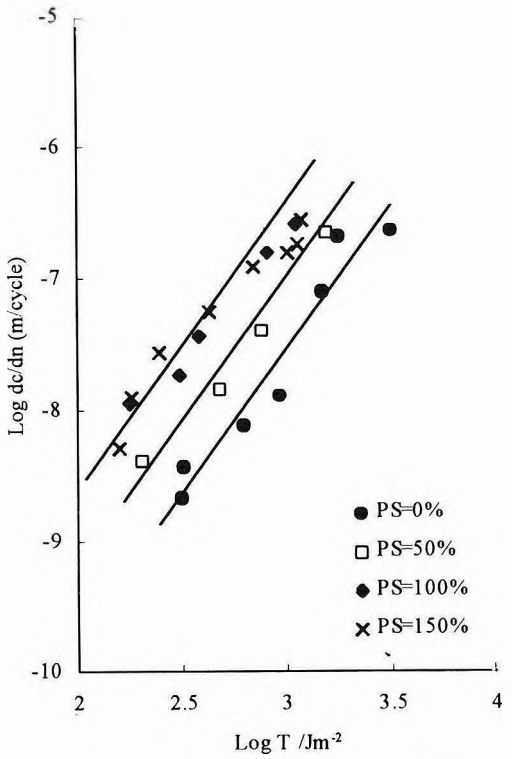

Figure 4. The crack growth rate versus *the tearing energy relationship for a variety of different pre-strains for material A.*

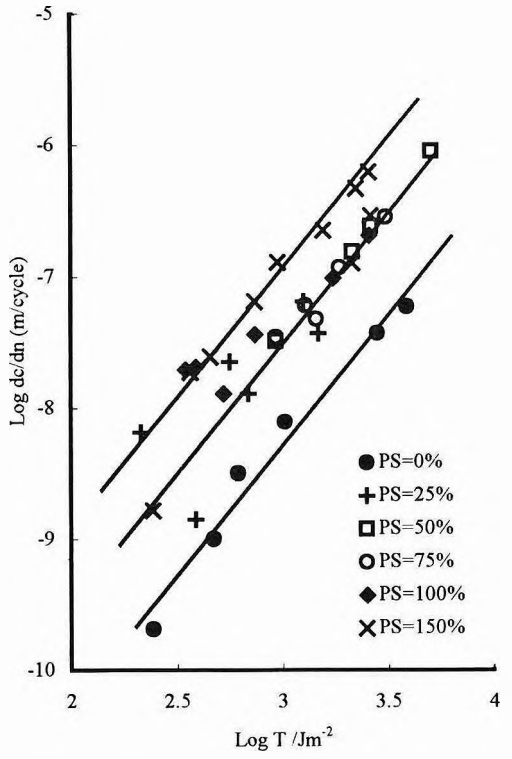

Figure 5. The crack growth rate versus *the tearing energy relationship for a variety of different pre-strains for material B.*

This can be contrasted with the tearing results reported by Gent and Kim[1] and A.B. Samsuri[2] where pre-strain showed a dramatic drop in the tear strength, especially in the case of filled rubbers.

Tear measurements have been made on the highly filled material C at a pre-strain of 75% with T values in the range of 1600 Jm^{-2}. The rate at which the crack propagates is broadly similar in time to the cyclic crack growth rate. This suggests that the behaviour in the upsweep region is dominated by a time dependent phenomenon.

Pre-stressing by 100% and 200% were carried out and the specimens were allowed to relax. The tearing energy *versus* crack growth results are plotted in *Figure 7.* These data are compared with the data from an un-strained specimen.

No significant differences are observed between the 3 sets of data. This indicates that the pre-stressing in the direction of the crack does not affect the strength of the specimen in that direction. These results are in contradiction with the tear measurements found in the literature. A possible explanation could be the

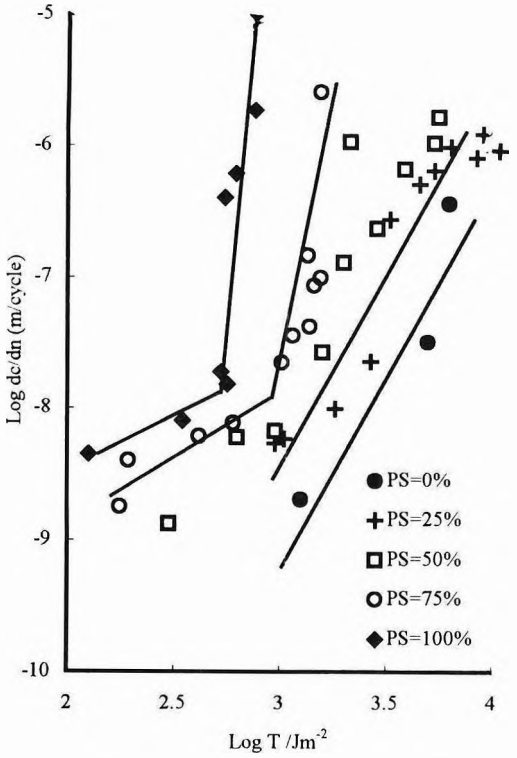

Figure 6. The crack growth rate versus *the tearing energy relationship for a variety of different pre-strains for material C.*

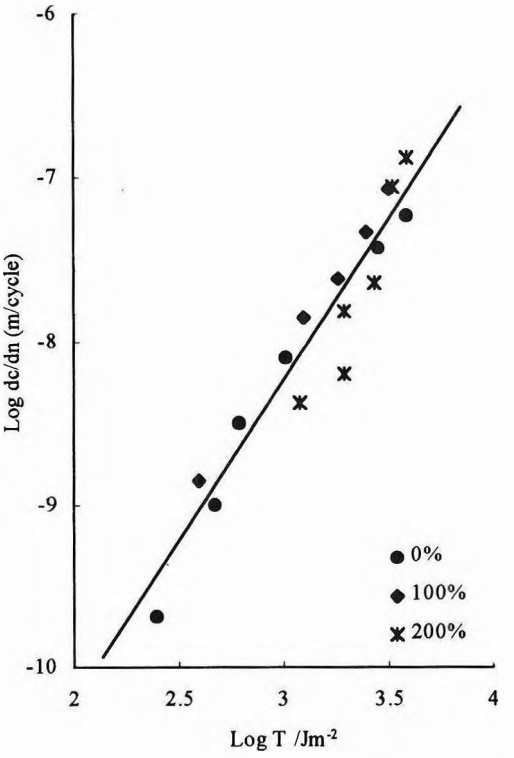

Figure 7. The effects of an orthogonal and relaxed pre-strain on the tearing energy versus *crack growth rate behaviour. Data is shown for tests performed without a pre-strain and with specimens that have had a previous pre-strain history of 100% and 200% strain applied.*

essential difference between these two experiments. Namely, the cyclic tests are not performed under continuous loading. This cyclic loading could to some extent reduce or even erase the anisotropy of strength in the direction of the crack. According to Gent and Kim[1], the pre-stressing caused the formation of an oriented region in the direction of the crack free of carbon black. This is due to segregation of rubber and carbon black when the rubber strain crystallises under the pre-stressing. One can reasonably say that the cyclic loading in the vertical direction would somehow produce the same effect and would probably re-establish an isotropy of strength, in a state close to the virgin state.

The same experiments realised on unfilled materials or non-strain crystallising elastomers would provide clarification of this phenomenon.

The fracture surfaces are investigated using SEM. The samples are sectioned perpendicular to the fracture surface, so that the crack profiles can be readily seen. The fractured surface is the upper surface shown on the photographs. The two photographs shown in *Figure 8* are both for compound C with a crack growth at 75% pre-strains. The two different tests correspond to different tearing energies. With

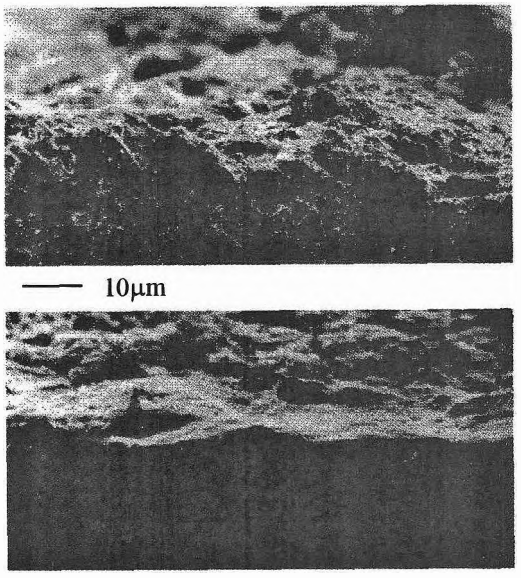

Figure 8. SEM photographs showing sectioned tearing face profile of material C with a pre-strain of 75% applied. In both photographs the tearing surface is the top face. The tearing energy and hence the crack growth rate are both higher in the upper photograph.

the upper photograph at 1000 Jm^{-2} there is a crack growth rate of 20 nm/cycle and with the lower photograph at 1600 Jm^{-2} there is a higher crack growth rate of 3000 nm/cycle. These points are respectively just below and above the breakpoint in characteristic crack growth behaviour, and correspond to a hundred fold increase in the crack growth rate. In the upper photograph at the lower tearing energy, the fracture surface is very rough and shows signs of considerable forking of the crack tip. This is reminiscent of incipient knotty tearing. The lower photograph shows a much smoother surface with no signs of crack forking at the resolution we are observing.

The pre-straining in the direction of the crack growth thus appears to inhibit the anisotropy development necessary to produce knotty tearing; thus under these circumstances the material is weak.

CONCLUSION

We have examined the effect of pre-straining on both the stress strain relationships and the tearing properties of filled natural rubber engineering compounds.

If it is assumed that W is a function of I_1 only then the stress strain behaviour for the pre-stressed sample can be predicted from the measured simple extension stress strain relationship. In general these predictions are in good accord with the measurements. A small discrepancy is observed for the higher pre-strains which is probably due to the breakdown and the reformation of the reinforcing filler structure. This will manifest itself as imperfect elastic behaviour.

The effect of pre-straining on the crack growth characteristics is to reduce the strength in the direction of the pre-strain by a factor ranging from three to eight depending on the amount of carbon black filler at a pre-strain of 100%. This behaviour is modified at higher tearing energies for the filler materials at pre-strains greater than about 75% when the time dependent crack growth rate increases by several orders of magnitude and then dominates the cyclic crack growth behaviour. This correlates with a marked change in the surface appearance from rough at the low rates of crack growth rate to smooth at the higher rates.

ACKNOWLEDGEMENTS

The authors are very grateful to BTR (AVS) for continued and generous support of this research.

REFERENCES

1. GENT, A.N. AND KIM, H.J. (1978) Tear Strength of Stretched Rubber. *Rubb. Chem. Technol.*, **51**, 35.

2. AZEMI B. SAMSURI (1989) Tear Strength of Filled Rubbers. Ph.D Thesis, London School of Polymer Technology, North London Polytechnic, UK.

3. GRIFFITH, A.A. (1921) The Phenomena of Rupture and Flow in Solids. *Philosophical Transcripts of the Royal Society*, **243**, 163.

4. RIVLIN, R.S. AND THOMAS, A.G. (1953) Rupture of Rubber. Part 1. Characteristic Energy for Tearing. *J. Polym. Sci.*, **10**, 291.

5. GREENSMITH, H.W. AND THOMAS, A.G. (1955) Rupture of Rubber. Part 3. Determination of Tear Properties. *J. Polym. Sci.*, **18**, 189.

6. THOMAS, A.G. (1960) Rupture of Rubber. Part 6. Further Experiments on the Tear Criterion. *J. Appl. Polym. Sci.*, **3**, 168.

7. LINDLEY, P.B. (1972) Energy for Crack Growth in Model Rubber Components. *J. Strain Anal.*, **7**, 132.

8. LINDLEY, P.B. AND TEO, S.C. (1979) Energy for Crack Growth at the Bonds of Rubber Springs. *Plastics and Rubber: Materials and Applications*, **4**, 29.

9. CHANG, Y.-W., GENT, A.N. AND PADOVAN, J. (1993) Strain Energy Release Rates for Internal Cracks in Rubber Blocks. *International Journal of Fracture*, **60**, 363.

10. DE, D.K. (1994) The Effect of Particulate Fillers on the Strain Energy Function and Crack Growth in Rubbers. Ph.D Thesis, Queen Mary & Westfield College, London University.

11. DAVIES, C.K.L., DE, D.K. AND THOMAS, A.G. (1994) Characterisation of the Behaviour of Rubber for Engineering Design Purposes. 1. Stress Strain Relations. *Rubb. Chem. Technol.*, **67**, 716.

12. YEOH, O.H. (1990) Characterisation of Elastic Properties of Carbon-Black Filled Natural Rubber Vulcanizates. *Rubb. Chem. Technol.*, **63**, 792.

13. TRELOAR, L.R.G. (1956) *Rheology*, Vol. 1. (*Eirich, F.R. ed.*) Ch. 10, 351. New York: Academic Press.

J. nat. Rubb. Res., **12(3)**, 142–153

Hyperelastic Material Models for Finite Element Analysis of Rubber[†]

O.H. YEOH[*]

Traditional design of rubber engineering components involves hand calculations assuming linear (Hookean) stress-strain behaviour. Such calculations are restricted to the simplest geometries and ignore the well-known non-linear stress-strain behaviour of rubber. Modern design methodology based on finite element analysis do not suffer from these limitations. However, the use of such computer-based techniques is hampered by difficulties in describing the stress-strain behaviour of rubber in the form of suitable hyperelastic material models. This is in spite of the fact that the underlying mathematics have been well developed by the pioneering efforts of Mooney, Rivlin, and Ogden.

This paper describes recent work that has yielded new perspectives of the Rivlin and Ogden hyperelastic material models. It suggests that rubber is best represented by a model where the shear modulus varies with strain in a relatively simple manner. While the approach has been developed as a practical solution to the problem of material characterisation for the purposes of finite element analysis, it has interesting repercussions in our interpretation of the molecular basis for rubber elasticity.

In the traditional method of designing rubber engineering components[1,2], the designer uses simple 'hand' calculations to estimate load-deflection characteristics and load-bearing capacity. To keep the calculations tractable, it is necessary to assume that the rubber material exhibits *linear* (Hookean) stress-strain behaviour, ignoring the well-known *non-linear* characteristics of rubber elasticity. Even so, such calculations are limited to the simplest of geometries and loading conditions. As a result, the calculations are at best only approximate and there are considerable reliance on experience and somewhat arbitrary 'rules of thumb'. This method produces rather conservative designs which have served us quite well up to now.

Today, however, the customer is constantly demanding more efficient designs. Modern components must be smaller, lighter, carry more load, serve under harsher environments, last longer, *etc.* and yet be cheaper than the part it replaces. Also, the ever shortening of the new product cycle means that there is less and less time available for multiple prototypes and extended testing. The traditional method of hand calculations is simply not accurate enough for us to get it right the first time. We need more accurate predictions of performance. We

[†] Paper presented at the International Rubber Conference 1997 Malaysia, 6–9 October, Kuala Lumpur

[*] Lord Corporation, Mechanical Products Division, 2000 West Grandview Boulevard, Erie, PA 16514-0038, U.S.A.

cannot ignore the non-linearity of rubber just to keep the mathematics simple.

Fortunately, intractable calculations can often be solved numerically. When engineers first applied finite element analysis (a computer-based technique for engineering analysis) to rubber design problems[3] in the early 1970s, only the largest universities and research institutes could afford the powerful computers needed to tackle even the simpler problems. Today, such computer facilities are readily available to everyone. So, it is no surprise to find that finite element analysis is fast becoming the normal method for designing rubber components.

But, computer hardware and finite element analysis software are not enough. They are merely tools for the skilled engineer which enable him to analyse the problem more accurately and quickly. There is no substitute for the skilled engineer's knowledge and understanding of his materials, processes, designs and service requirements. We shall only discuss one facet of the materials knowledge base here; the stress-strain properties of rubber.

Finite element analysis of rubber components requires as input a mathematical description of the stress-strain properties of the material. This usually takes the form of a strain energy function sometimes referred to as a 'hyperelastic material model'. Characterisation of a specific rubber material consists of performing stress-strain measurements followed by curve-fitting the data. Finite element analysis programs even provide utilities for the regression analysis. However, the task is not as trivial as it seems. Inadequate material models are often the cause of lack of agreement between finite element analysis predictions and experiment. This paper is intended to serve as a practical guide to the novice on how reasonable, even if approximate, material models may be obtained from a limited testing program.

THEORETICAL FOUNDATIONS

Material models may be derived from two separate approaches to the study of rubber elasticity: (a) the statistical or kinetic theory; and (b) the phenomenological theory.

Statistical Theory

According to the Statistical Theory of Rubber Elasticity[4], the non-linear stress-strain behaviour of rubber may be derived from molecular considerations to yield the constitutive equation:

$$W = C_{10}(I_1 - 3) \qquad \ldots 1$$

where W is the strain energy density, C_{10} is a material constant which is related to molecular parameters, and I_1 is the first invariant of the Green deformation tensor. *Equation 1* is commonly known as the neo-Hookean material model. Unfortunately, this model is only valid for a relatively small range of strains[4]. Many attempts have been made to refine the basic Statistical Theory. These yield increasingly complex constitutive models but none have found practical utility in finite element analysis. Nevertheless, the Statistical Theory occupies a central position in our understanding of the molecular basis of rubber elasticity.

Phenomenological Theory

Mooney[5] took the phenomenological approach which treats the problem from the continuum mechanics viewpoint. Assuming that

the rubber is homogenous, isotropic, elastic, incompressible and obeys Hooke's law in simple shear, he obtained the strain energy function:

$$W = C_{10}(I_1 - 3) + C_{01}(I_2 - 3) \qquad \ldots 2$$

where C_{10} and C_{01} are material constants and I_1 and I_2 are the first two invariants of the Green deformation tensor. *Equation 2* is usually quite successful in describing tensile data up to moderately large strains of about 100%. However, it is significantly less successful in other modes of deformation, especially compression. In spite of this limitation, it is probably the most commonly used material model in the finite element analysis of rubber. Although Mooney's phenomenological approach makes no appeal to molecular theory, it is common to identify C_{10} with molecular parameters in the Statistical Theory and to interpret C_{01} as a measure of deviations from the theory perhaps reflecting a failure to achieve equilibrium conditions[6].

Rivlin[7] considerably expanded and generalised Mooney's approach and showed that the most general strain energy function for a homogenous, isotropic, incompressible, elastic material is:

$$W = \sum_{i+j=1}^{n} C_{ij}(I_1 - 3)^i (I_2 - 3)^j \qquad \ldots 3$$

The first order approximation of this power series is identical to *Equation 2* which became popularly known as the Mooney-Rivlin model.

More recently, another material model due to Ogden[8] appears to be gaining popularity. Ogden's strain energy function may be written as:

$$W = \sum_{p=1}^{n} \frac{\mu_p}{\alpha_p}(\lambda_1^{\alpha_p} + \lambda_2^{\alpha_p} + \lambda_3^{\alpha_p} - 3) \qquad \ldots 4$$

where μ_p and α_p are material constants and λ_1, λ_2, and λ_3, are the principal extension ratios. In the Ogden formulation, the indices, α_p, need not be integers.

We note that the Rivlin and Ogden material models are, power series and so it appears possible to fit experimental stress-strain data to any desired degree of precision by merely taking a sufficient number of terms. Therefore, these material models are in principle better than the two-constant Mooney-Rivlin model. Indeed, it is a common fallacy to assume that the more terms in the strain energy function, the better. In practice, the additional degrees of freedom introduced by extra terms allow the regression analysis to do a better job of fitting experimental errors in the stress-strain data! The result is often unstable strain energy functions which predict physically unrealistic behaviour under conditions outside the range of experimental data[9–11]. Indeed, higher order strain energy functions usually show such poor ability to predict behaviour outside the range of experimental data that Chow and Cundiff[11] recommended the use of the Mooney-Rivlin material model. Clearly, its simplicity and robustness are so valued that its inaccuracies are tolerated.

According to Rivlin and Sawyers[12], the Ogden model is a special case of the Rivlin strain energy function. Treloar[4] expressed the opinion that the two formulations were essenially equivalent and that the choice of one over the other is simply a question of convenience. So, from the viewpoint of performing finite element analysis, it does not matter which strain energy function is used so long as it gives an adequate representation of

the material properties with a reasonable number of fitting coefficients. The question that remains is how the coefficients of the chosen material model may be obtained from a modest testing program.

RECENT DEVELOPMENTS

One difficulty common to both the Rivlin and Ogden material models is the fact that they contain a number of arbitrary fitting constants of uncertain physical significance. So long as we regard the development of material models merely as a curve-fitting exercise, it is difficult to determine when an adequate model has been derived and further refinements are not justified. We review here some recent work which has shed new light on the underlying physics of these models. Armed with this new understanding, the development of realistic material models is seen to be significantly simplified.

Rivlin's Formulation

We start by considering a material obeying Rivlin's model (*Equation 3*) subjected to simple shear deformation. The shear stress, τ, is related to the amount of shear, γ by[4]:

$$\frac{\tau}{\gamma} = 2\left[\frac{\partial W}{\partial I_1} + \frac{\partial W}{\partial I_2}\right] \qquad \ldots 5$$

It is seen that the shear modulus is given by the sum of the partial derivatives $\partial W/\partial I_1$ and $\partial W/\partial I_2$. For the specific cases of the neo-Hookean and Mooney-Rivlin material models, $\partial W/\partial I_1$ and $\partial W/\partial I_2$ are constants; that is the shear modulus is constant. However, in the more general Rivlin material model, $\partial W/\partial I_1$ and $\partial W/\partial I_2$ are functions of I_1 and I_2. We note from *Equation 5* that it is impossible to evaluate the individual values of $\partial W/\partial I_1$ and $\partial W/\partial I_2$ from shear stress-strain data. In fact, Kawabata and Kawai[13] have pointed out that it is impossible to evaluate $\partial W/\partial I_1$ and $\partial W/\partial I_2$ from stress-strain data from any single mode of deformation; it is necessary to have data from two or more modes of deformation. This increases considerably the amount of experimental work needed to characterise the rubber.

A considerable simplification is possible. Gregory[14] had noted that usually $\partial W/\partial I_1$ is much larger than $\partial W/\partial I_2$. So, Yeoh[15] suggested assuming $\partial W/\partial I_2 = 0$. This simplifies Rivlin's material model to:

$$W = \sum_{i=1}^{\infty} C_{ij}\,(I_1 - 3)^i \qquad \ldots 6$$

where j is always zero but has been retained for consistency with Rivlin's nomenclature. The shear modulus, τ/γ, is then given by:

$$\frac{\tau}{\gamma} = 2\frac{\partial W}{\partial I_1} = 2C_{10} + 4C_{20}\,(I_1 - 3) + 6C_{30}\,(I_1 - 3)^2 + \ldots. \qquad \ldots 7$$

Recalling that the shear strain is related to I_1 by[4]:

$$\gamma^2 = (I_1 - 3) \qquad \ldots 8$$

it is seen that Yeoh's model implies a material whose shear modulus varies with even powers of the amount of shear. This is consistent with the symmetry of the deformation.

Figure 1 shows the dependence of shear modulus on $(I_1 - 3)$ for a typical unfilled natural rubber vulcanisate. We find that at small strains, the shear modulus decreases with increasing

strain but at large strains, the shear modulus increases with increasing strain. A convenient way to describe this strain dependence of shear modulus is the relation[16,17]:

$$\frac{\tau}{\gamma} = 2A \exp\left[-B(I_1 - 3)\right] + 2C_{10} + 4C_{20}(I_1 - 3) + 6C_{30}(I_1 - 3)^2 + \ldots \quad \ldots 9$$

which implies the strain energy function:

$$W = \frac{A}{B}\left\{1 - \exp\left[-B(I_1 - 3)\right]\right\} + \sum_{i=1}^{\infty} C_{ij}\,(I_1 - 3)^i \quad \ldots 10$$

Since the exponential term may be written as a polynomial, it is seen that *Equations 9* and *10* are not really different from *Equations 7* and *6*. But this particular form has the advantage of implying two mechanisms; the exponential term reflects the small strain behaviour where the shear modulus decreases with increasing strain while the polynomial term reflects the large strain behaviour where the shear modulus increases with increasing strain.

Expressing the strain energy function in terms of $(I_1 - 3)$ alone, simplifies the problem of material characterisation considerably since it is no longer necessary to evaluate $\partial W/\partial I_1$ and $\partial W/\partial I_2$ at fixed values of I_2 and I_1, respectively. Also, since $\partial W/\partial I_2$ is now irrelevant, data from any single deformation mode is sufficient. Regression analysis using shear data is obvious from the above discussion but the more readily available tensile data may be used instead[15]. Thus, it is possible to develop appropriate strain energy functions to describe elastic behaviour of rubbers from a limited test program[15,16]. Strain energy functions of this form (*Equations 6* and *10*) have been used successfully in finite element analysis[18–20].

Ogden's Formulation

Here, we seek some physical interpretation of the material parameters, μ_p and α_p. For simplicity and compact printing, we shall consider an Ogden strain energy function with just one term and accordingly will drop the subscript in the following. The arguments can be easily extended to Ogden models with *n* terms since each term has the same form.

We start by considering simple shear deformation. It can be readily shown[21] that the secant shear modulus is given by:

$$\frac{\tau}{\gamma} = \frac{2G_0}{\alpha}\left(\frac{\lambda^{\alpha} - \lambda^{-\alpha}}{\lambda^2 - \lambda^{-2}}\right) \quad \ldots 11$$

where G_0 is the small strain shear modulus, and λ is the extension ratio of the equivalent pure shear deformation which is related to the amount of shear, γ by:

$$\gamma = \lambda - \lambda^{-1} \quad \ldots 12$$

Equation 11 shows that the secant shear modulus is a function of α and of the shear strain (which is reflected in λ). The form of the dependence is shown in *Figure 2* where the shear stress, τ, is plotted as a function of shear strain, γ, for materials with a small strain shear modulus, G_0, equal to 1 MPa but with different values for the index α. It is seen that when α takes the value of 2 (*i.e.* the material is neo-Hookean), the shear stress-strain curve is linear (*i.e.* the shear modulus is constant). When α is *less* than 2, the material *softens* with increasing strain. On the other hand, when

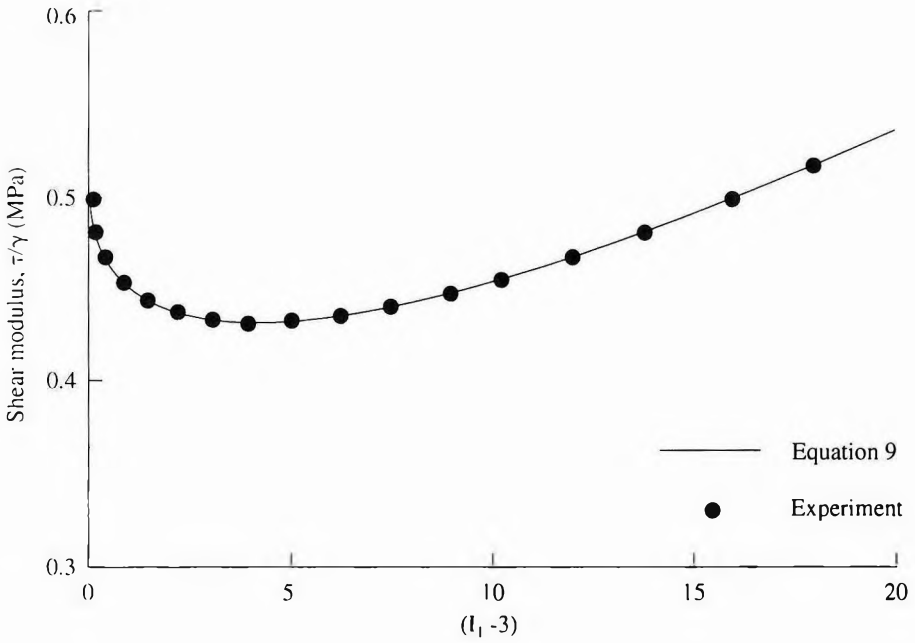

Figure 1. Strain dependence of shear modulus for typical unfilled natural rubber vulcanisate.

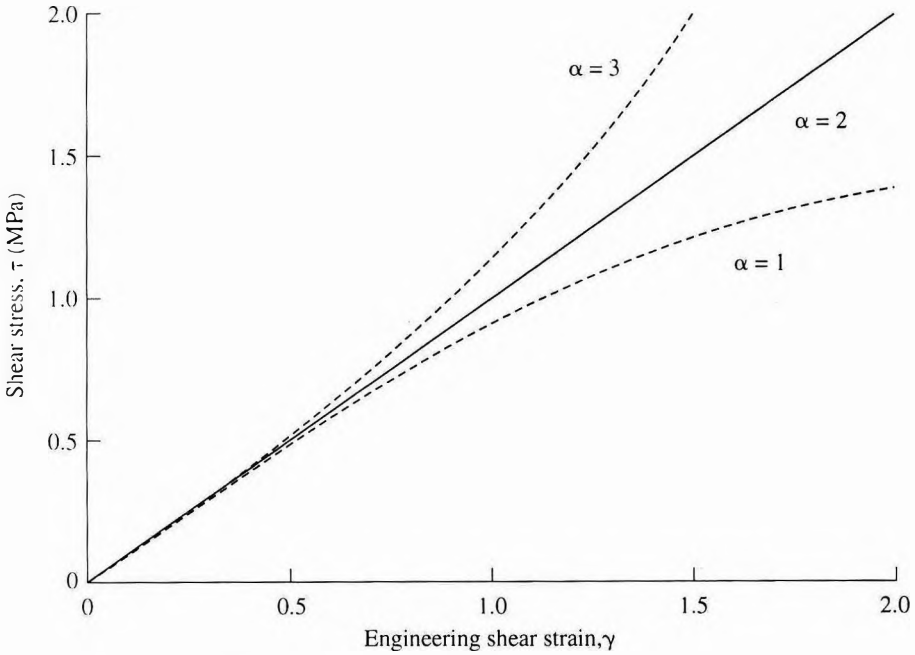

Figure 2. Simple shear stress-strain curves for Ogden materials with different values of α.

α is *greater* than 2, the material *stiffens* with increasing strain. The form of *Equation 11* is such that the same behaviour is obtained when α takes a negative value; it is the absolute value of α which determines whether the shear modulus decreases or increases with increasing strain. Although this dependence of shear modulus on α is intrinsic to the Ogden strain energy function, it is strange that there appears to be no comment about this in the literature.

When we consider Ogden material models with $n > 1$, we note that the product $\mu_p \alpha_p$ each makes a contribution to the shear modulus and that G_0 is given by:

$$G_0 = \sum_{p=1}^{n} \frac{\mu_p \alpha_p}{2} \qquad \ldots 13$$

For the Mooney-Rivlin material model, $\alpha_1 = 2$ and $\alpha_2 = -2$. From the above we find that the shear modulus of the Mooney-Rivlin model is constant. This, of course, is no surprise since Mooney[5] started with the assumption that the stress-strain curve of rubber is linear in simple shear. When $|\alpha_p| < 2$, that term's contribution to the secant shear modulus decreases with increasing strain and conversely, when $|\alpha_p| > 2$, that term's contribution to the shear modulus increases with increasing strain. So, the shear stress-strain curve of a multi-term Ogden material will meander to a greater or lesser degree depending on the relative magnitudes of α_p and μ_p.

Ogden suggested that stress-strain data for an unfilled natural rubber vulcanisate reported by Treloar[22] may be represented by an Ogden material model with the coefficients:

$\alpha_1 = 1.3$, $\mu_1 = 0.618$ MPa
$\alpha_2 = 5.0$, $\mu_2 = 0.00118$ MPa
$\alpha_3 = -2.0$, $\mu_3 = -0.00981$ MPa

From the above, it is now clear what Ogden's model implies. The first term ($\alpha_1 = 1.3$) indicates that the shear modulus *decreases* with increasing strain. The relatively large value of μ_1 means that this term dominates behaviour at small strain. The second term ($\alpha_2 = 5.0$) indicates that the shear modulus *increases* with increasing strain and this term will dominate behaviour at large strains. The third term ($\alpha_3 = -2.0$) reflects on relative contributions to tensile and compressive stresses when the deformation deviates from shear[21]. The relatively small value of μ_3 means that this term is not very significant and neglecting it is equivalent to the neglect of the $(I_2 - 3)$ by Yeoh. Thus, taken together, Ogden's model describes the same general dependence of shear modulus on strain we discussed earlier.

IMPLICATIONS FOR MOLECULAR THEORY

Although our primary motivation for the study of the phenomenological theory of rubber elasticity is the development of material models to facilitate finite element analysis, we cannot help but reflect upon the implications for the molecular theory. A material model with arbitrary coefficients remains nothing more than a curve-fit unless we are able to relate the coefficients to some fundamental principle. Some recent attempt has been made in this direction.

We note that the elementary Statistical Theory leading to *Equation 1* assumes Gaussian chain statistics which are invalid as the chains approach their fully extended state at large

strains. More elaborate theories have been developed taking into account the finite extensibility of the chains. Specifically, Langevin chain statistics have been invoked[4]. Wang and Guth[23] showed that consideration of finite chain extensibility leads to additional, higher order terms in I_1 and I_2. Unfortunately, the resulting strain energy function depends on the specifics of the molecular model and the number of terms in the material model makes it difficult to make direct comparisons between theory and experiment.

Recently, Gent[24] suggested a new strain energy function which may be written as:

$$W = -C_{10}\,(I_m - 3)\,\ln\left[1 - \frac{(I_1 - 3)}{(I_m - 3)}\right] \qquad \ldots 14$$

where I_m is the limiting value of I_1 corresponding to the deformation when the network is fully stretched. The logarithmic term may be written as a polynomial, so *Equation 14* is of the form of *Equation 6*. Ignoring I_2 terms may be partly justified on the grounds that at least in the cases of certain molecular network models proposed by Wang and Guth[23] and Arruda and Boyce[25], strain energy functions have been derived which contain only terms in I_1. *Equation 14* predicts a shear modulus which increases with increasing strain. This is consistent with observed behaviour at large strains. So, it appears that the increase in modulus with increasing strain is associated with finite chain extensibility.

Gent's strain energy function has the advantage of reducing rubbery stress-strain behaviour to just two closely related parameters which, moreover, have clear physical meaning in molecular terms. The constant I_m is the limiting value of I_1 corresponding to the deformation when the network is fully-stretched. So I_m is related to chain length and inversely related to crosslink density. Recalling from the Statistical Theory that C_{10} is proportional to crosslink density, we see that I_m is inversely proportional to C_{10}.

Recently, Yeoh and Fleming[17] extended Gent's treatment and suggested that the same parameters have significance at small strains too. They suggested writing the strain energy function in the form:

$$W = \frac{A}{B}\,(I_m - 3)[1 - \exp(-BR)] - C_{10}\,(I_m - 3)\ln(1 - R) \qquad \ldots 15$$

where:

$$R = \frac{(I_1 - 3)}{(I_m - 3)} \qquad \ldots 16$$

and presented supporting experimental data. They tested a family of four unfilled natural rubber vulcanisates which differ in crosslink density. *Figure 3* shows that $(I_m - 3)$ is inversely proportional to C_{10} as expected from Gent's theory. Also, the stress-strain behaviour of all four rubbers in different deformation modes may be predicted from measurements made on just one member in a single mode. This is illustrated in *Figure 4* where the tensile stress-strain curve of one member, shown as a solid line, has been fitted to *Equation 15* and the derived material coefficients have been used to predict the behaviour of the entire family under different deformation modes. The predictions are shown in *Figures 4–6* as broken

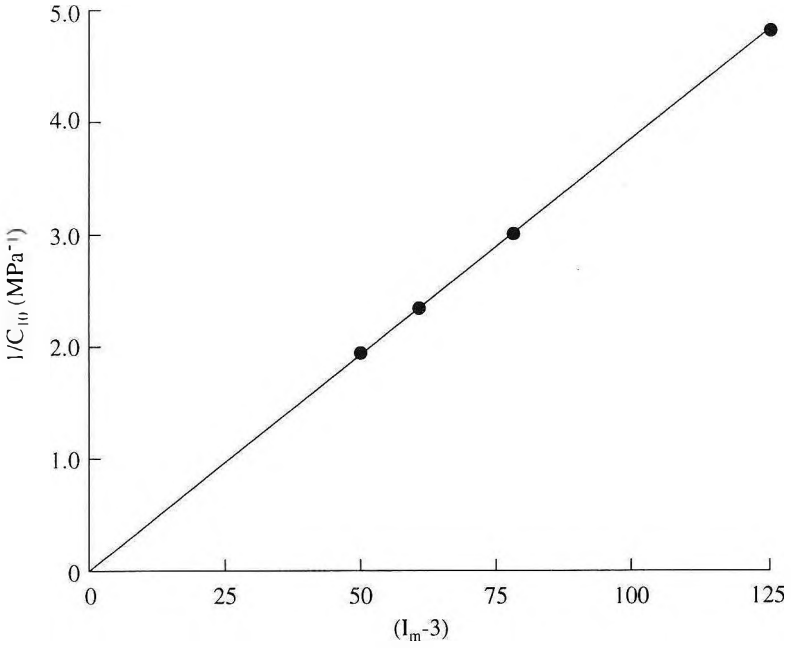

Figure 3. Relation between (I_m-3) *and* $1/C_{10}$.

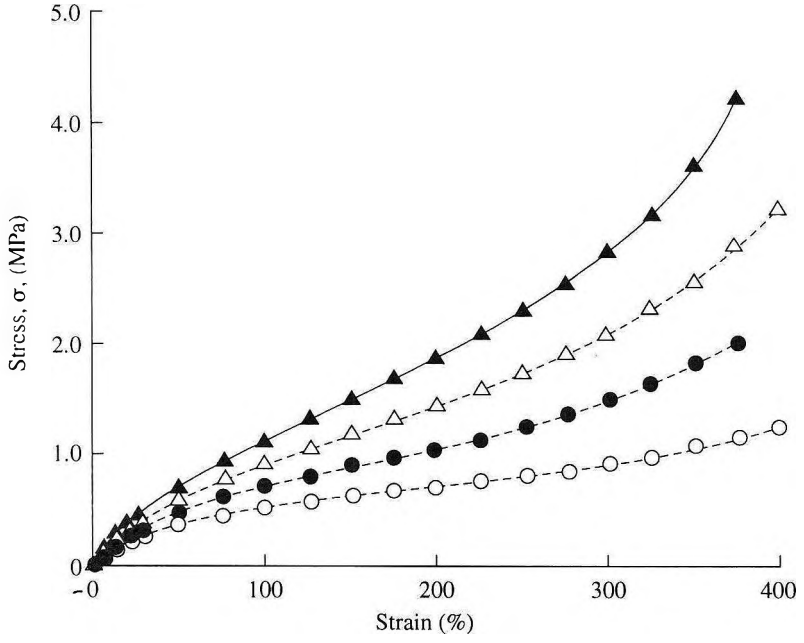

Figure 4. Comparison of theory with experiment. Simple extension.

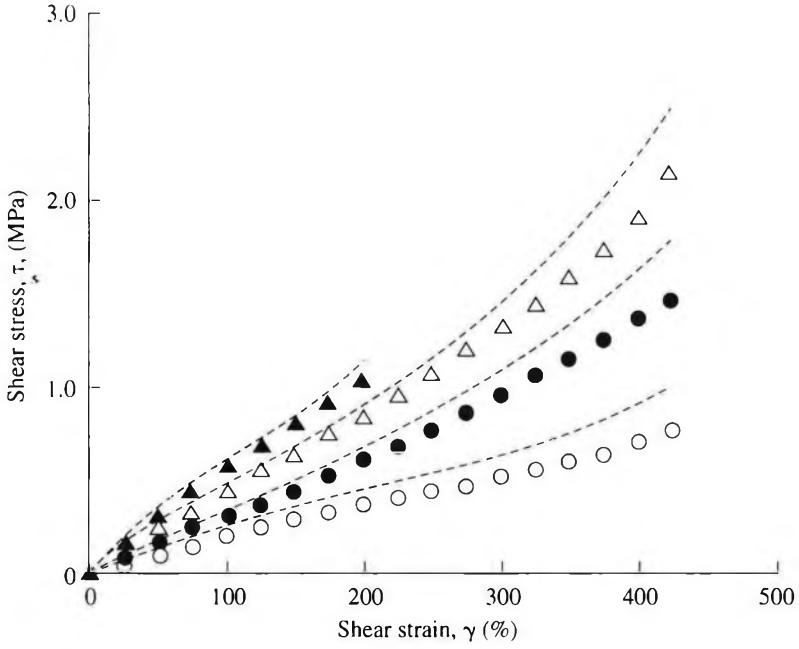

Figure 5. Comparison of theory with experiment. Simple shear.

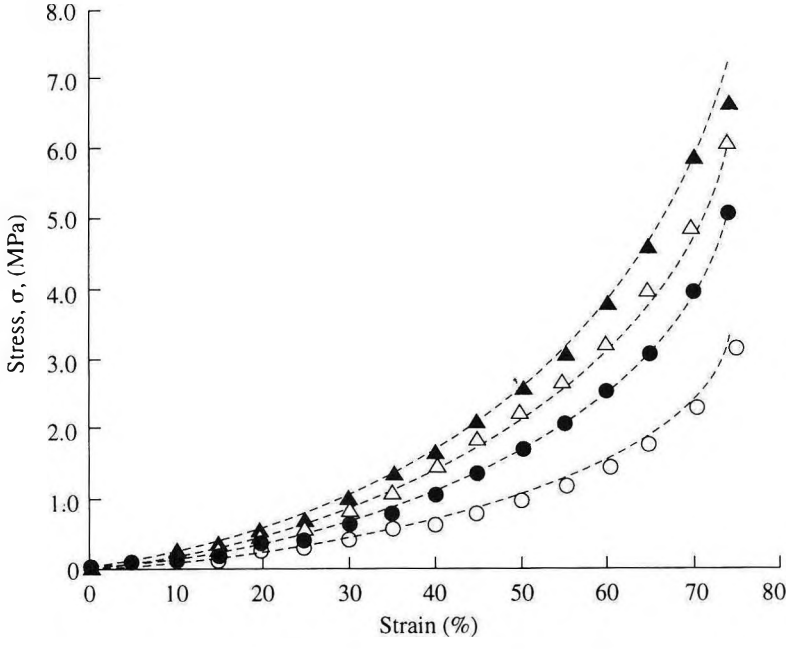

Figure 6. Comparison of theory with experiment. Compression between lubricated plates.

lines. It is seen that the agreement between theory and experiment is quite satisfactory.

CONCLUSIONS

We conclude that the stress-stain properties of rubber is best represented by a model where the shear modulus varies with strain in a relatively simple manner. At small strains, the shear modulus *decreases* with increasing strain. At large strains, the shear modulus *increases* with increasing strain. This insight has facilitated the development of practical material models for finite element analysis.

This approach has interesting repercussions in our interpretation of the molecular basis for rubber elasticity. We regard the model from classical Statistical Theory as our basic model with two mechanisms for enhancement of shear modulus. At large strains, the shear modulus increases because of finite chain extensibility. At small strains, the source of shear modulus enhancement is less obvious. Empirically, we know that it decreases rapidly from a finite value as strain increases. We speculate that it may be related to network defects. Unlike previous treatments which interpret deviations from the Statistical Theory in terms of the second Mooney constant (*i.e.* in terms of I_2), we attribute all deviations to additional terms in I_1.

REFERENCES

1. LINDLEY, P.B. (1974) Engineering Design with Natural Rubber. *Technical Bulletin*, Malaysian Rubber Producers' Research Association, Brickendonbury, England.

2. FREAKLEY, P.K. AND PAYNE, A.R. (1978) *Theory and Practice of Engineering with Rubber.* London: Applied Science.

3. LINDLEY, P.B. (1973) *Proc. Intl. Rubb. Conf., Brighton, May 1972.* London: Institution of the Rubber Industry.

4. TRELOAR, L.R.G. (1975) *The Physics of Rubber Elasticity*, 3rd ed. Oxford: Clarendon Press.

5. MOONEY, M. (1940) *J. Appl. Phys.*, **11,** 582.

6. KRIGBAUM, W.R. AND ROE, R-J (1965) *Rubb. Chem. Technol.*, **38,** 1039.

7. RIVLIN, R.S. (1956) Large Elastic Deformations. *Rheology: Theory and Applications*, (*Eirich, F.R. ed.*) Vol. 1. N.Y.: Academic Press.

8. OGDEN, R.W. (1972) *Proc. R. Soc. Lond.*, **A 326,** 565.

9. JAMES, A.G., GREEN, A. AND SIMPSON, G.M. (1975) *J. Appl. Polym. Sci.*, **19,** 2033.

10. JAMES, A.G. AND GREEN, A. (1975) *J. Appl. Polym. Sci.*, **19,** 2319.

11. CHOW, C.L. AND CUNDIFF, C.H. (1987) *Tire Sc. Technol.*, **15,** 73.

12. RIVLIN, R.S. AND SAWYERS, K.N. (1976) *Trans. Soc. Rheo.*, **20,** 545.

13. KAWABATA, A. AND KAWAI, H. (1977) *Adv. Polym. Sci.*, **24,** 89.

14. GREGORY, M.J. (1979) *Plast. Rubber Mater. Appl.*, **4,** 184.

15. YEOH, O.H. (1990) *Rubb. Chem. Technol.*, **63,** 792.

16. YEOH, O.H. (1993) *Rubb. Chem. Technol.*, **66,** 754.

17. YEOH, O.H. AND FLEMING, P.D. (1997) *J. Polym. Sci., Part B*, **35,** 1919.

18. CHEN, J.S., SATYAMURTHY, K. AND HIRSCHFELT, L.R. (1994) *Computer and Structures*, **50,** 715.

19. CHEN, J.S. AND PAN, C. (1996) *J. Appl. Mechanics*, **68,** 862.

20. CHEN, J.S., WU, C.T. AND PAN, C. (1996) *J. Appl. Mechanics*, **68,** 869.

21. YEOH, O.H. (1997) *Rubb. Chem. Technol.*, **70,** 175.

22. TRELOAR, L.R.G. (1994) *Trans. Faraday Soc.*, **40,** 59.

23. WANG, M.C. AND GUTH, E. (1952) *J. Chem. Phys.*, **20,** 1144.

24. GENT, A.N. (1996) *Rubb. Chem. Technol.*, **69,** 59.

25. ARRUDA, E.M. AND BOYCE, M.C. (1993) *J.Mech. Phys. Solids*, **41,** 389.

J. nat. Rubb. Res., **12(3)**, 154–165

Determination of the Molecular Architecture of Synthetic and Natural Rubber by the Use of Thermal Field-flow Fractionation and Multi-angle Laser Light Scattering†

W.S. FULTON*# AND S.A. GROVES*

The processability of elastomers is largely governed by molecular architecture and hence the influence of molecular weight distribution, branching and gel content is of great interest. Analysis by conventional size exclusion chromatography (SEC) has limitations which may distort the molecular weight distribution. However, the combination of Thermal Field Flow Fractionation (ThFFF) and Multi-angle Laser Light Scattering (MALLS) has allowed absolute molar mass and size distribution to be obtained without the need for calibration, standards or assumptions. ThFFF is a separation technique that enables the physical structure and composition of complex macromolecules to be determined and relies on diffusive transport as the principal mechanism of separation. An open channel geometry minimises shear effects, making it possible to separate fragile, high molecular weight polymers, whilst the absence of a stationary phase means that adsorption effects can be ignored. Consequently, complex mixtures of polymer, micro-gel and macro-gel can be studied in a single run without the need for filtration. By combining all the information derived from ThFFF/MALLS a more comprehensive molecular weight distribution, including levels of branching, can be determined. Light scattering profiles and absolute molecular weight distributions were determined by ThFFF/MALLS for a number of synthetic and natural rubbers and comparisons have been made with results obtained from conventional SEC. For example, the molecular weight distribution of natural rubber has been shown to extend up to 10^9 g/mol with approximately 20% of the rubber having a molecular weight greater than 10^7 g/mol. MALLS can also provide information on the size distribution of species and this is discussed further in relation to both synthetic and natural rubber.

It is well known that the rheological properties of rubber, like any polymer melt, are greatly affected by variations in molecular weight distribution and branching. Production techniques, for both synthetic and natural rubber, will influence molecular architecture; more so for synthetic rubber where deliberate modification creates material specific properties. Therefore, it is of great practical importance to understand how the fundamental

† Paper presented at the International Rubber Conference 1997 Malaysia, 6–9 October, Kuala Lumpur

* Tun Abdul Razak Research Centre, Brickendonbury, Hertford, SG13 8NL, United Kingdom

Corresponding author

structure of rubber molecules, including branching, effects processability and final product performance.

Certain elastomers have molecular weight distributions with tails that extend beyond 10^7 g/mol, *i.e.* above the exclusion limit of the majority of size exclusion chromatography (SEC) columns. Rubber in solution may also contain a significant gel component and this is routinely separated prior to injection onto a SEC column, making analysis of the true molecular weight distribution virtually impossible. Also many high molecular weight polymers are fragile and easily susceptible to shear degradation that may occur in SEC columns. Such degradation will cause a downward shift of molecular weight distribution from that of the original material, again making subsequent analysis unreliable.

Field-flow fractionation (FFF) is a series of separation techniques that has been applied to many macromolecular and colloidal systems. As with conventional SEC, FFF is a flow-elution method in which differential retention is achieved by application of an external field or gradient perpendicular to a narrow, ribbon-like flow channel. This technique was first developed by Prof. J. Calvin Giddings[1] and uses an open channel for separation, making it possible to separate macro-molecules and particles ranging in size from 5 nm (or 10^3 g/mol) to 100 μm.

Thermal Field-flow Fractionation (ThFFF)

ThFFF is a variety of FFF in which a temperature gradient is used as the field. The theory of ThFFF has been developed and refined by several workers[2–4] and is briefly reviewed here.

In ThFFF, separation is achieved by applying a temperature gradient (10^4 °C.cm^{-1}) across a thin (127 μm) ribbon-like channel through which a polymer solution flows *(Figure 1)*. The temperature gradient drives polymer molecules towards the cold or accumulation wall by the process of thermal diffusion. The concentration of molecules due to thermal diffusion is opposed by mass diffusion and at equilibrium a solute zone is formed whose concentration profile decreases exponentially from the cold wall. The fundamental mechanism of separation is provided by the velocity profile across the thin dimension of the channel; velocity is fastest in the centre and slowest at the two walls. Consequently, the distance between the cold wall and the solute zone governs the rate at which the zone travels through the channel. Polymers are separated because constituent molecules of different size attain equilibrium at different distances from the cold wall; smaller molecules sited further from the cold wall travel faster and are eluted first. Therefore the subsequent fractogram describes an elution sequence which proceeds from low to high molecular weight.

The general retention equation for isoviscous and parabolic flow that describes the elution order for each component from the channel is:

$$R = \frac{t^\circ}{t_r} = \frac{V^\circ}{V_r} = 6\lambda\left\{\coth\frac{1}{2\lambda} - 2\lambda\right\} \qquad \ldots 1$$

where R is the retention ratio, t_r and V_r are the elution time and volume for a given component, V° is the channel void volume and t° is the time for non-retained samples to elute. The retention parameter λ is defined as:

$$\lambda = \frac{l}{w} \qquad \ldots 2$$

where 1 is the solute thickness and w is the channel thickness. The retention parameter for ThFFF is given by:

$$\lambda = \frac{D}{D_T \Delta T} \quad \ldots 3$$

where D is the ordinary diffusion coefficient, D_T is the thermal diffusion coefficient and ΔT is the difference in temperature between the hot and cold walls. D_T is virtually independent of chain length and branching, whereas D has a molecular weight *(M)* dependence of the following form for random coil polymers:

$$D = \Phi M^{-n} \quad \ldots 4$$

which because of the lack of dependence of D_T upon M can be written as:

$$\log\left\{\frac{D}{D_T}\right\} = \log\lambda\Delta T = \log\Phi - n\log M \quad \ldots 5$$

where Φ and n are empirical constants. Such an equation serves as the basis for calibrating elution volume (or time) to molecular weight.

Multi-angle Laser Light Scattering (MALLS)

MALLS is an analytical technique derived from classical methods for determining absolute molecular weight and size. Unlike traditional detectors, the MALLS photometer has eighteen discrete photo-detectors spaced around a flow cell in a special geometry, ensuring that measurements may be made simultaneously over a broad range of angles, typically 15° – 160°, depending on solvent/glass refractive indices *(Figure 2)*. The unique electro-optical configuration, combined with use of a flow cell, enables this detector to be coupled to a variety of separation systems, such as a ThFF Fractionator.

The intensity of scatter can be directly related to the molecular weight of polymer, and the root mean square radius of gyration according to *Equations 6* and *7*[7]:

$$\frac{K^* c}{R(\theta)} = \frac{1}{[M_w P(\theta)]} + 2A_2 c \quad \ldots 6$$

where $R(\theta)$ is the excess Rayleigh light scattering factor, M_w is the weight average molar mass, $P(\theta)$ is the scattering function, A_2 is the second virial coefficient and

$$K^* = \frac{4\pi^2 n_o^2 (dn/dc)^2}{\lambda_o^4 N_A} \quad \ldots 7$$

where n_0 is the refractive index of the solvent, *dn/dc* is the specific refractive index increment, λ_0 is the wavelength of laser light and N_A is Avogadro's number. The scattering function $P(\theta)$ is related to the radius of gyration (R_g) by the following relation:

$$P(\theta) = \left[1 + \frac{16\pi^2}{3\lambda^2} \langle R_g^2 \rangle \sin^2\left\{\frac{\theta}{2}\right\}\right] \quad \ldots 8$$

To determine molecular weight for a given elution slice, the scattering is plotted as a function of angle and extrapolated back to zero angle. The intercept value is then used to determine the absolute molecular weight of each monodisperse slice, while the slope of the line gives an independent measure of root mean square radius of gyration *(Figure 3)*. Data for each slice are combined to produce a series of distribution plots for the sample as a whole,

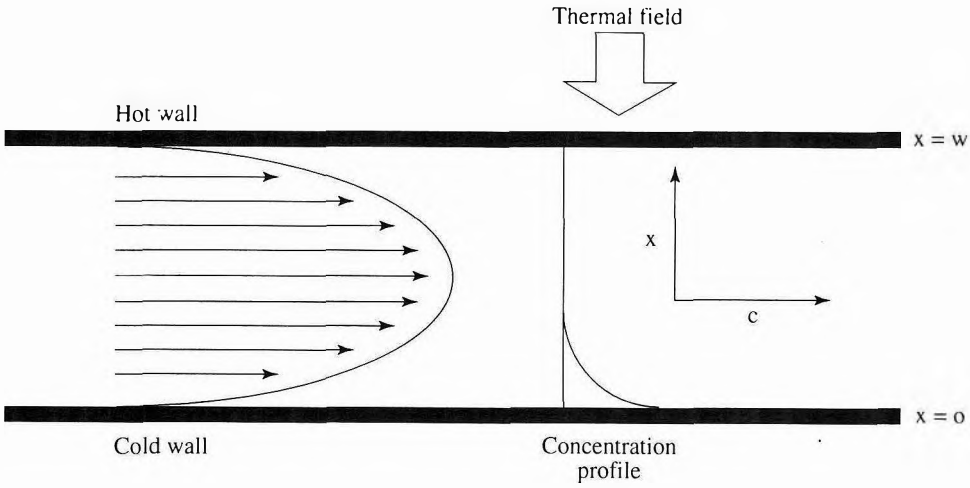

Figure 1. Principles of ThFFF separation.

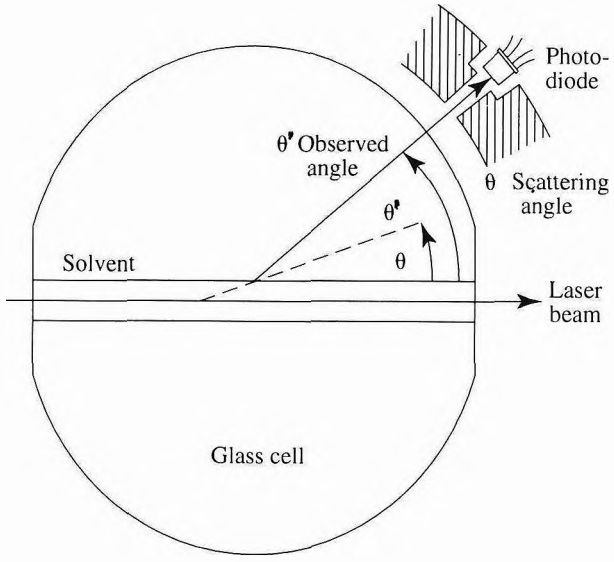

Figure 2. Scattering geometry of MALLS flow cell.

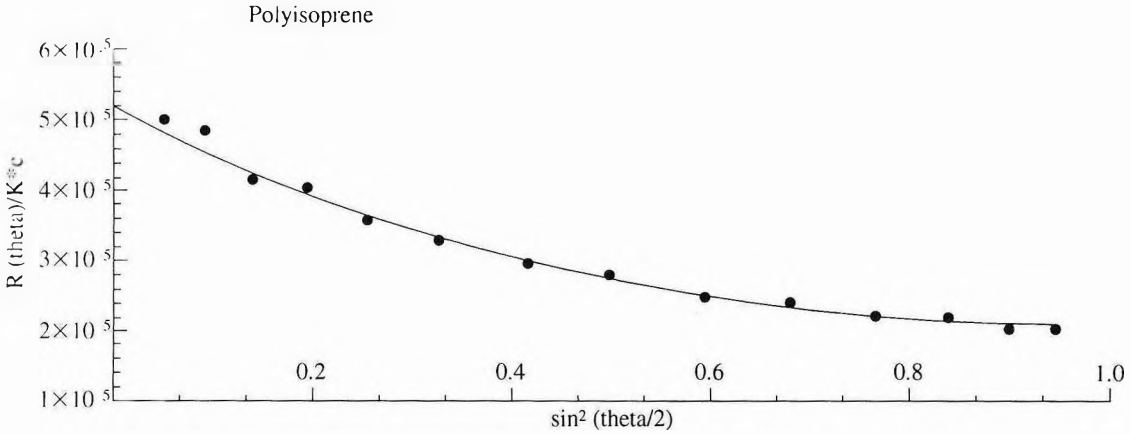

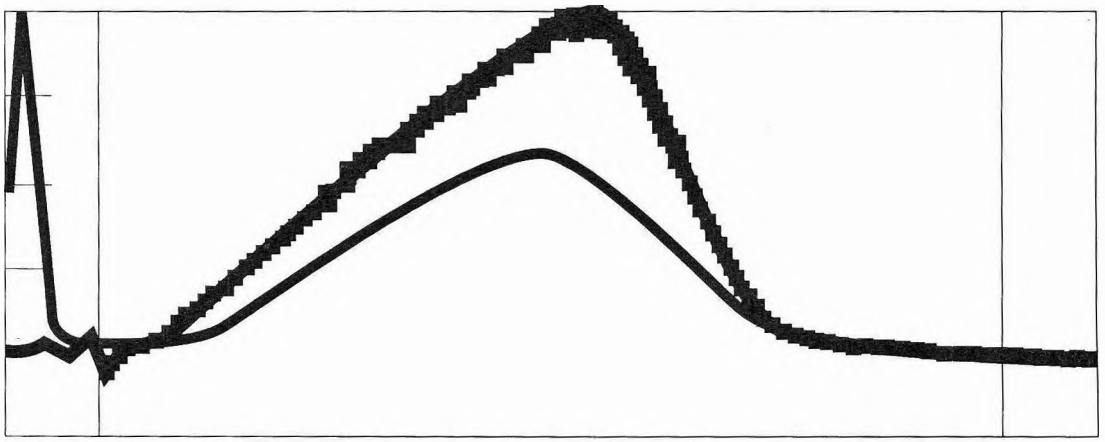

90° and AUX detectors

Peak. Slice : 1,3080
Volume : 8.778 mL
Fit degree : 2
Conc. : (2.087 ± 0.001) e-5 g/mL
Mw : (5.167 ± 0.091) e+5 g/mol
Radius : 69.4 ± 2.2 nm

Figure 3. Typical Debye plot obtained from the MALLS software.

providing absolute size distributions and absolute molecular weight. By defining the relationship between size and molecular weight, essential parameters can be derived, including molecular conformation and the extent of long-chain branching.

EXPERIMENTAL

The rubbers used in this study were *Cariflex IR305* (Shell), *Natsyn 2200* (Goodyear), Natural rubber (SMR L) and BR (Europrene Neo-*cis* BR40, 98% *cis*-1,4 poly(butadiene), Enichem). Samples were dissolved in HPLC grade cyclohexane (Sigma-Aldrich Chemical Company), which was also used as carrier solvent in the ThFFF channel. Samples (1.0 – 2.0 mg/ml) were introduced into the channel *via* an injection valve fitted with a 20 µL loop.

The ThFFF system was a Polymer Fractionator Model T100 manufactured by FFFractionation Inc, (Salt Lake, Utah, USA). The channel comprised of two nickel plated copper bars with highly polished surfaces separated by a Teflon coated polyimide spacer, 46 cm long (tip-to-tip), 2 cm wide and 127 µm thick. The lower bar was cooled with circulating water and the upper bar heated by two 1.5 kW heater elements. The channel was pressurised to approximately 100 p.s.i. to elevate the boiling point of the carrier solvent. ΔT, the initial temperature gradient across the channel, was set between 50°C and 80°C, depending on the rubber, and programmed to decay over a given period of time. This so-called, 'power programming' enabled separation of low molecular weight species from the void peak at a high initial ΔT. Then the programme slowly released the thermal field allowing high molecular weight polymer to move towards the centre of the channel and into faster moving fluid elements. Consequently, complete fractionation was achieved in a reasonable time (up to one hour). A Waters 515 HPLC pump was used for solvent delivery. The channel effluent was detected by a DuPont 2310 variable wavelength ultra-violet detector (at 215 nm) and a Wyatt DAWN DSP multi-angle laser light scattering detector at 633 nm. The measured flow rate of the mobile phase through the system was 0.171 ml/min.

The SEC analyses were performed on a set of Polymer Laboratories Mixed-B columns using THF at a flow rate of 0.75 ml/min and a temperature of 40°C; nominal concentration was about 5 mg/ml in all cases. The detector utilised UV light at 215 nm. The instrument was calibrated with polystyrene standards.

RESULTS/DISCUSSION

Figure 4 shows the size exclusion chromatograms obtained from filtered solutions of *Cariflex IR305* and *Natsyn 2200*. The molecular weight distributions are essentially similar with a peak molecular weight of 500 000.

For classical FFF, molecular size increases across the distribution and *Figure 5* shows a typical plot of radius of gyration *versus* elution volume. The concentration profile is overlaid to show how molecular size varies from 30 nm to 130 nm across the distribution. The fractogram illustrates the expected separation mechanism by which the smallest molecules are eluted first, the converse of SEC. *Figure 6* shows the differential molecular weight and size distribution derived from the previous fractogram *(Figure 5)*. The slope of the double logarithmic plot of radius of gyration *versus*

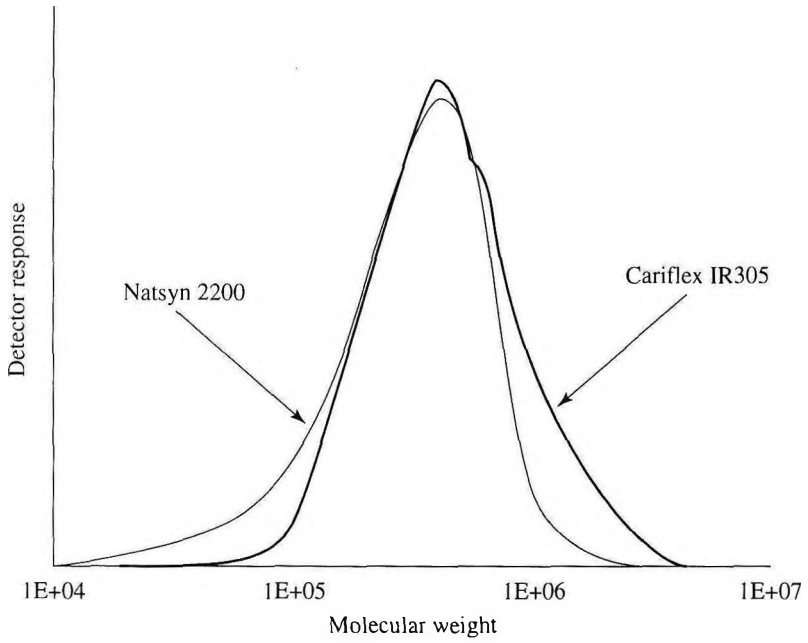

Figure 4. Molecular weight distribution of Natsyn 2200 *and* Cariflex IR305 *obtained by SEC.*

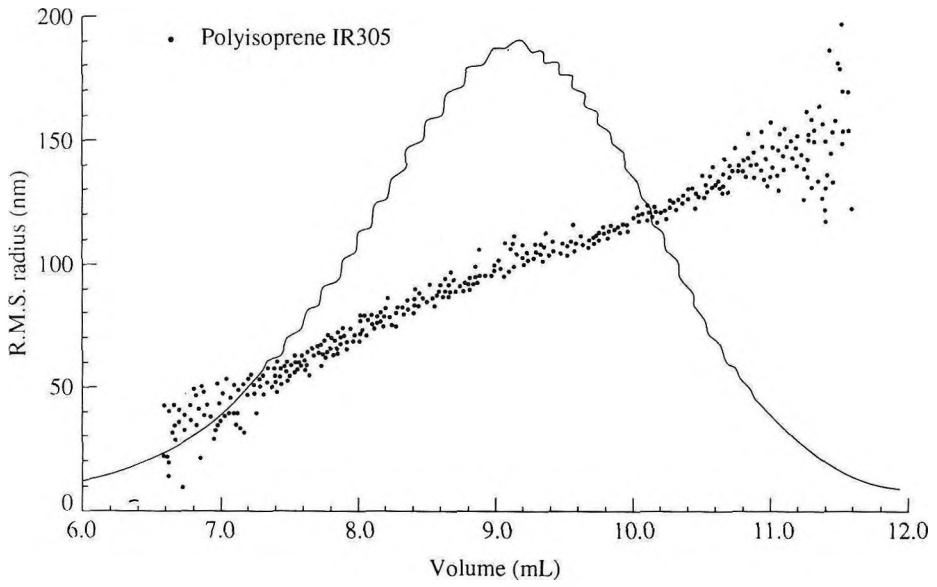

Figure 5. Fractogram showing the size based separation of IR305. The UV concentration profile is also shown.

molecular weight indicates the type of molecular conformation that polymer chains adopt in solution[8,9]. Random, linear polymer coils, in good solvents, have slopes in the range 0.5 – 0.6. Branched molecules may have slopes smaller than a value typical of a random coil, making the change of slope a measure of the extent of long-chain branching. The slope calculated from data shown *(Figure 6)* was approximately 0.5. This would indicate that IR305 was comprised essentially of linear molecules throughout the molecular weight distribution. Analysis of the polyisoprene, *Natsyn 2200*, yielded results *(Figure 7)* in which the molecular weight distribution was much broader than IR305, extending to a value of 10^7 g/mol and where the slope of radius of gyration *versus* molecular weight changed from approximately 0.5 to 0.3 at about $5x10^5$ g/mol. It seems reasonable to assign the limiting line with a slope of 0.3 to branched species and the one with a slope of 0.5 to linear polymer chains. Interpretation of such results would suggest that polymer below a molecular weight of $5x10^5$ g/mol is linear and that above is branched, with the extent of branching increasing with increasing molecular weight. *Natsyn 2200* contained an appreciable gel content (25% w/v in THF) which, because of filtration prior to injection, would not be analysed *via* conventional SEC. Conversely, all the elastomer was injected onto the ThFFF channel and so a more comprehensive analysis of the molecular weight distribution and conformation emerged by the combination of ThFFF/MALLS. Such an analysis also throws light on how molecular conformation is dependant on the stereo-specific catalyst systems used for the synthesis of these two polyisoprenes[10], *i.e.* Zeiger-Natta type catalysis for *Natsyn 2200* and lithium-anionic catalysis for IR305.

Figure 8 shows the dependence of radius of gyration on elution volume for *cis*-BR40 and the size-volume relation does not exactly follow the trend expected. This relationship can be explained with the occurrence of large gel species (500 nm – 600 nm) which eluted in the first 0.5 mL, after which normal separation took place. Increasing the physical size of the rubber molecule brings another mechanism of fractionation (Steric FFF) into play at a point defined as steric inversion. At this point of separation forces are larger and diffusion, which is strongly suppressed, no longer plays a major role in retention. Large particles are driven to the accumulation wall by the thermal field and are stopped by the physical barrier of the wall. Thus equilibrium elevation of the particle depends upon its size. Larger particles project further into the flow than their smaller counterparts and so they are literally 'bowled along' more rapidly. Consequently, large particles elute before small particles, opposite to that expected *via* classical fractionation. It is also likely that large particles co-eluted with low molecular weight species at the beginning of ThFFF separation. If so, the measured radius of gyration was an average value obtained for a particular elution slice and would mean that the actual size of gel particles was much larger, possibly greater than 1 μm.

Characterisation of natural rubber (SMR L) also revealed how steric inversion affects the molecular weight profile at the initial portion of the distribution *(Figure 9)*, where a mixture of species were co-eluted. The high molecular weight material eluting at the end of the separation has a molecular weight more than an order of magnitude greater than would be calculated from conventional SEC. Combination of these two effects will increase the measured molecular weight of natural

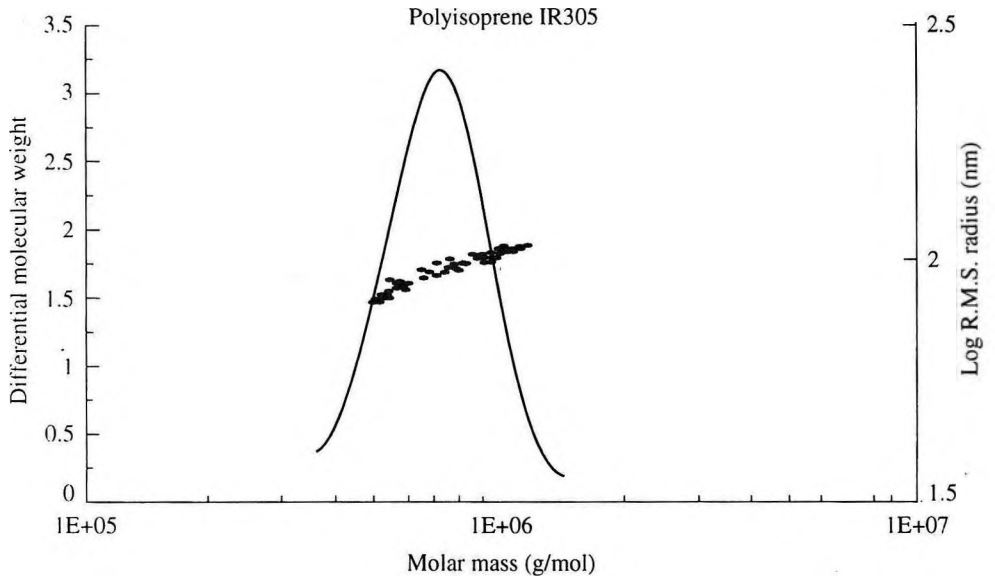

Figure 6. Differential molecular weight and radius of gyration as a function of molar mass for Cariflex IR305.

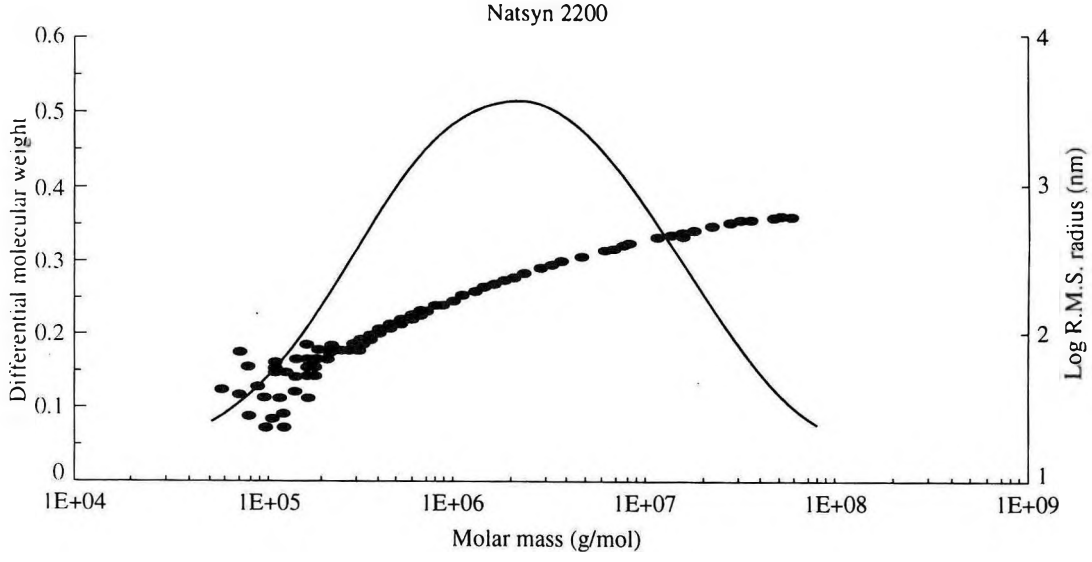

Figure 7. Differential molecular weight and radius of gyration as a function of molar mass for Natsyn 2200.

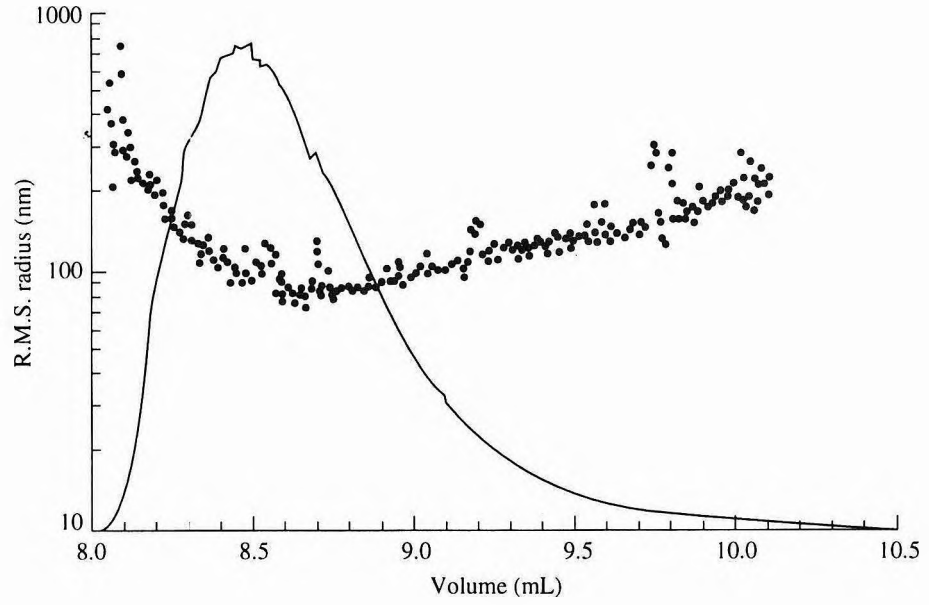

Figure 8. Fractogram of cis-*BR40 showing the size distribution through the light scattering profile.*

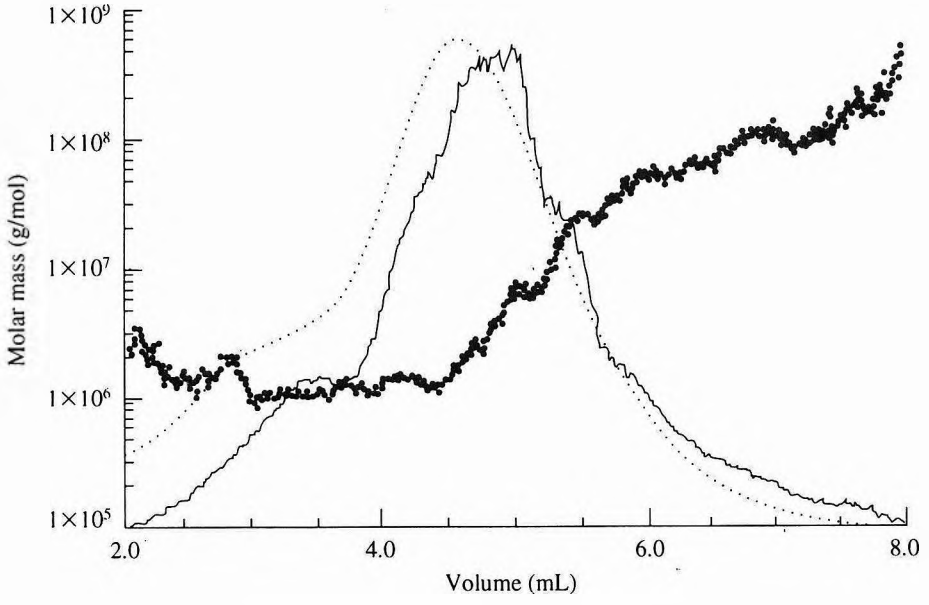

Figure 9. Molecular mass versus *elution volume for SMR L. Solid line denotes light scattering profile and dotted line denotes UV concentration profile.*

rubber from a few million to many tens of millions. The dependence of the radius of gyration on molecular weight is shown in *Figure 10* and size data below a molecular weight of 10^6 g/mol may be affected by possible co-elution. Nevertheless, the slope of the plot from 10^6 g/mol to 3 x 10^7 g/mol is 0.3 and can be attributed to star-shaped or branched molecules. The slope of radius of gyration *versus* molecular weight depends on the segmental density of polymer species. Above 3 x 10^7 g/mol the slope tends to zero, an indication of the presence of microgel particles which are much denser than polymer coils.

A recent and only characterisation[11] of natural rubber by ThFFF relied solely upon synthetic linear polyisoprene standards for calibration to derive an apparent molecular weight distribution. It was recognised that the amount of information obtained by this method was limited and so there was a perceived need for an absolute measure of molecular weight, such as that now obtained by a ThFFF/MALLS system.

CONCLUSION

This paper has demonstrated how complex mixtures of linear, branched and gel species

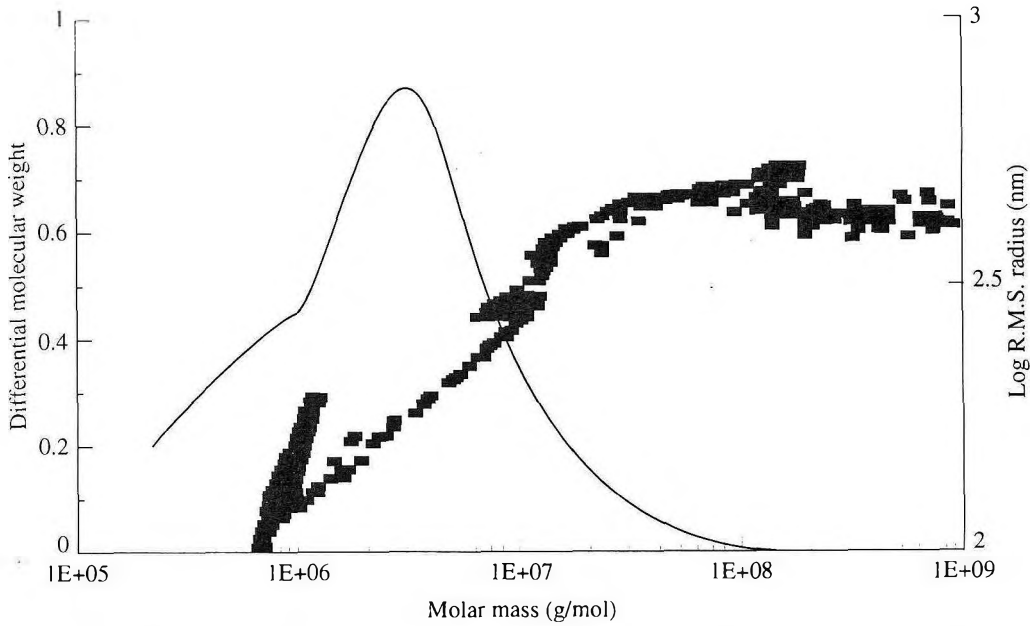

Figure 10. Differential molecular weight and radius of gyration as a function of molar mass for SMR L.

found in many elastomers can be studied without filtration. The novel combination of two powerful techniques, ThFFF and MALLS, has provided a system with distinct advantages over conventional SEC. The synergy between the two techniques provides a measure of absolute molecular weight and radius of gyration from which parameters such as long chain-branching can be derived.

REFERENCES

1. GIDDINGS, J.C. (1993) *Science*, **260**, 1456.

2. HOVINGH, M.E., THOMPSON, G.E. AND GIDDINGS, J.C. (1970) *Anal. Chem.*, **42**, 195.

3. GUNDERSON, J.J., CALDWELL, K.D. AND GIDDINGS, J.C. (1984) *Sep. Sci. Technol.*, **19**, 667.

4. MYERS, M.N., CALDWELL, K.D. AND GIDDINGS, J.C. (1974) *Sep. Sci.*, **9**, 419.

5. MYERS, M.N., CHEN, P. AND GIDDINGS, J.C. (1993) *Chromatography of Polymers: Characterization by SEC and FFF. ACS Symposium Series 521*, 47.

6. SCHIMPF, M.E. (1996) *Trends Polym. Sci.*, **4**, 114.

7. WYATT, P. (1993) *Anal. Chim. Acta*, **272**, 1.

8. DAVIDSON, N.S., FETTERS, L.J., FUNK, W.G., *et al.* (1987) *Macromolecules*, **20**, 2614.

9. TSUNASHIMA, Y., HIRATA, M., NEMOTO, N. *et al.* (1988) *Macromolecules*, **21**, 1107.

10. SENYEK, M.L. (1987) *Encyclopaedia of Polymer Science and Engineering*, **8**, 487.

11. LEE, S. AND MOLNAR, A. (1995) *Macromolecules*, **28**, 6354.

J. nat. Rubb. Res., **12(3)**, 166–175

Measurements of Total Extractable Proteins in Latex Gloves: A Comparative Study of the RRIM and ASTM *Tests*†

ESAH YIP*

Extractable protein contents of latex gloves generated by two commonly used methods, the RRIM (MS 1392:96P) *and the* ASTM (D 5712-95) *modified Lowry tests, were examined and their relationship studied.*

Total extractable proteins, EP_{RRIM}, determined by the RRIM test, ranged from 1326 μg/g to < 20 μg/g for 90 gloves. Their corresponding EP_{ASTM} values, obtained by the ASTM test, varied from 1377 μg/g to < 50 μg/g. Statistical analysis showed a very significant correlation between them , with a coefficient of correlation, $r = 0.93$, $P < 0.001$. Generally, EP_{RRIM} values read higher than those of EP_{ASTM}. EP_{ASTM} of 50 μg/g and lower were found to be associated with EP_{RRIM} values ranging from 267 μg/g to < 20 μg/g, suggesting higher sensitivity of the latter measurements. Relevance of the two sets of EP in relation to the allergenicity/allergic potential of latex gloves was discussed.

Accelerated ageing at 70°C for 7 days of latex gloves resulted in the lowering of protein contents. The effect appeared to be more pronounced for EP_{RRIM}, than for EP_{ASTM}.

In view of the latex protein allergy problem related to NR latex products, especially gloves[1], there is a need to evaluate the allergic potential of these products. However, till to-date, a universally standardised test for doing so is still lacking. Many different methods[2–9] are being used in various laboratories in different parts of the world. The methods most commonly adopted in manufacturing countries, particularly Malaysia, are the RRIM test (which has recently become a *Malaysian Standard Test*)[7] and the *ASTM* test[8], both for the determination of total extractable protein content of latex products.

While the RRIM test has been employed for as long as the beginning of the allergy problem, the *ASTM* was established a few years later. It is often asked how different the two sets of values so obtained are and if they are correlated. The present study has therefore been undertaken to compare these values and to see if any relationship exists between them. Furthermore, in view of the ageing requirement

† Paper presented at the International Rubber Conference 1997 Malaysia, 6–9 October, Kuala Lumpur

* Rubber Research Institute of Malaysia, P.O. Box 10150, 50908 Kuala Lumpur

by the FDA for 'Low Protein Labelling Claim' for latex gloves[10], this effect on total extractable proteins is also investigated.

MATERIALS AND METHODS

Preparation of Gloves Pieces

Square pieces, of dimension 7 cm x 7 cm, were cut from palm area of each glove sample. Care was taken to avoid any contamination.

Accelerated Ageing

Glove pieces were subjected to accelerated ageing at 70°C for 7 days, according to *ASTM 3578-91*.

RRIM Modified Lowry Test[7] (*Malaysian Standard Protein Test, MS 1392-96P*)

Cut pieces of each test sample were extracted in 0.01 *M* phosphate buffered saline (pH 7.4) at 23°C for 3 h. Extract was clarified by centrifugation, to sediment any particulate matter, such as powder. Precipitation of proteins was carried out using trichloroacetic and phosphotungstic acids. This was followed by further centrifugation at 10 000 × g for 30 min. The resulting pellet was redissolved in 0.2 *M* sodium hydroxide, and their concentration determined by the Lowry microassay. Absorbance readings, recorded at 750 nm, were calibrated against standard bovine serum albumin (BSA). Results were expressed as EP_{RRIM} in μg/g of gloves.

ASTM Protein Test[8]

Proteins were extracted in distilled water at 37°C for 2 h. Extract was centrifuged and the proteins were precipitated using deoxycholate, trichloroacetic and phosphotungstic acids. Sedimentation of the protein pellet was carried out by centrifugation at 6000 x g for 15 min. The precipitated proteins were redissolved in 0.01 *M* sodium hydroxide, and their concentration determined by Lowry microassay according to procedure set out in the BioRad *DC* protein kit. Absorbance was recorded at 750 nm and readings calibrated against standard ovalbumin. Results were presented as EP_{ASTM}, in μg/g of gloves.

RESULTS

Total Extractable Protein Contents

A total of 90 commercial gloves were extracted and tested using both the RRIM and *ASTM* methods. Results are summarised in *Table 1*. It can be seen that total extractable protein content, EP_{RRIM}, ranged from as high as 1326 μg/g to as low as to 19 μg/g. Their median and overall mean values were 505 μg/g and 519 μg/g, respectively. Similarly, values of EP_{ASTM}, varied from 1377 μg/g to 36 μg/g, with a median of 372 μg/g and a mean of 423 μg/g. Comparison of the overall means indicated EP_{ASTM} was 18.5% lower than that of the EP_{RRIM}, while in the case of the medians, the decrease was 26.3%.

Closer examination of the data at different EP_{RRIM} ranges, revealed that means of EP_{ASTM} read 13.8% – 25% lower than those of EP_{RRIM} when the latter values were greater than 100 μg/g. However, at EP_{RRIM} of 100 μg/g and lower, the mean of EP_{ASTM} indicated 17.6% higher values than that of EP_{RRIM} (*Table 2*).

Comparison of data based on different EP_{ASTM} ranges, on the other hand, was found to vary somewhat as shown in *Table 3*. Although

TABLE 1. COMPARISON OF EXTRACTABLE PROTEIN CONTENTS BY RRIM AND *ASTM* METHODS FOR 90 GLOVE SAMPLES

Item	EP_{RRIM} (μg/g)	EP_{ASTM} (μg/g)	% diff.
Range	19 – 1326	36 – 1377	–
Median	505	372	26.3
Mean	519	423	18.5
S.d.	407	348	–

S.d.: Standard deviation

TABLE 2. MEANS OF EP_{RRIM} AND EP_{ASTM} AT DIFFERENT EP_{RRIM} RANGES FOR 90 GLOVE SAMPLES

EP (μg/g)	EP_{RRIM} range (μg/g)				
	100 & less	>100 – 400	>400 – 700	>700 – 1000	>1000
No. of samples	20	21	16	18	15
Corresponding EP_{ASTM} Range	36–107	49–408	219–673	360–1377	557–1238
EP_{RRIM} Mean (S.d.)	51 (28)	212 (63)	551 (86)	846 (83)	1148 (102)
EP_{ASTM} Mean (S.d.)	60 (23)	159 (106)	451 (120)	729 (228)	877 (184)
% diff [a]	–17.6	25.0	18.1	13.8	23.6

[a] % with reference to EP_{RRIM} values

lower EP_{ASTM} values than those of EP_{RRIM} were still apparent, the difference was more marked at the lower ranges. Nevertheless, statistical analysis of the two sets of data showed that they are very closely related, with the coefficient of correlation, $r = 0.93$, $P < 0.001$ (*Figure 1*).

Effect of Accelerated Ageing

EP_{RRIM} and EP_{ASTM} contents of latex gloves were determined with and without accelerated ageing. Of the 77 lots of commercial gloves tested, 61 were powdered gloves, and 16 were powder-free of which 4 were siliconised,

TABLE 3. MEANS OF EP_{RRIM} AND EP_{ASTM} AT DIFFERENT EP_{ASTM} RANGES FOR 90 GLOVE SAMPLES

EP (μg/g)	EP_{ASTM} range (μg/g)				
	50 & less	>50 – 100	>100 – 400	>400 – 700	>700
No. of samples	14	16	19	21	20
Corresponding EP_{RRIM} Range	19–206	51–267	113–835	434–1017	817–1326
EP_{RRIM} Mean (S.d.)	66 (71)	136 (79)	353 (142)	743 (167)	1065 (162)
EP_{ASTM} Mean (S.d.)	45 (6)	76 (18)	289 (83)	576 (82)	924 (178)
% diff.[a]	31.8	44.1	18.1	22.5	13.2

[a] % with reference to EP_{RRIM} values

3 polymer coated and the rest chlorinated. Results are summarised in *Table 4* below.

It is apparent that accelerated ageing resulted in a lowering of 25.2% in the overall means of EP_{RRIM} and 16.5% reduction in the corresponding EP_{ASTM} measurements. The magnitude of changes was relatively greater in the case of the powdered gloves (reduction of 25.4% in EP_{RRIM}, and 16.9% in EP_{ASTM}), and less so in the powder-free gloves (10.6% and 4.2%, respectively).

The aged EP values were very well related to those of the unaged in both cases, especially the EP_{RRIM}, as illustrated in *Figures 2* and *3*. The higher coefficient of correlation of 0.98 for EP_{RRIM} as compared to 0.92 for EP_{ASTM} (both at $P < 0.001$) supports the higher sensitivity of the RRIM test.

DISCUSSION

Total Extractable Proteins

Although both the RRIM and *ASTM* tests involved the Lowry colorimetric assay technique, their protocols are not the same. Briefly, the general procedure comprises three parts: (1) Protein extraction, (2) Protein precipitation and (3) Protein quantitation. A number of variations have been adopted by both tests (*Appendix 1*). These have consequently resulted in differences not only in the sensitivity of the tests, but also in the extractable protein (EP) values so generated. This is particularly so in the case of the calibration curves, where absorbance readings are much lower for the *ASTM* test than the RRIM test for the same protein concentration. Sensitivity limits of the methods are, in fact, 20 μg/g and 50 μg/g for the RRIM and the *ASTM* tests, respectively. In agreement with

TABLE 4. EFFECT OF ACCELERATED AGEING ON EP_{RRIM} AND EP_{ASTM} OF LATEX GLOVES

Glove samples	EP_{RRIM} (μg/g)			EP_{ASTM} (μg/g)		
	Unaged	Aged	% change	Unaged	Aged	% change
All gloves (n = 77)						
Range of EP	5 – 1540	3 – 1186		14 – 1966	8 – 1537	
Mean EP	591	442	– 25.2	484	404	– 16.5
Powdered gloves (n = 61)						
Range of EP	33 – 1540	21 – 1186		48 – 1966	25 – 1537	
Mean EP	733	547	– 25.4	598	497	–16.9
Powdered-free gloves (n = 16)						
Range of EP	5 – 140	3 – 121		14 – 159	8 – 130	
Mean of EP	47	42	–10.6	48	46	– 4.2

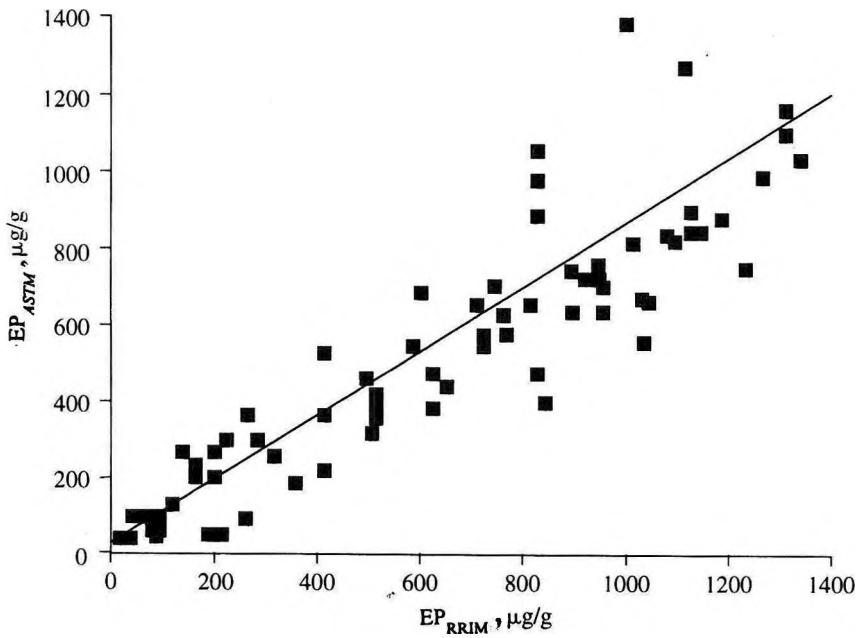

Figure 1. Correlation between EP_{RRIM} and corresponding EP_{ASTM} values of latex gloves. Coefficient of correlation, r = 0.93, P<0.001, n = 90.

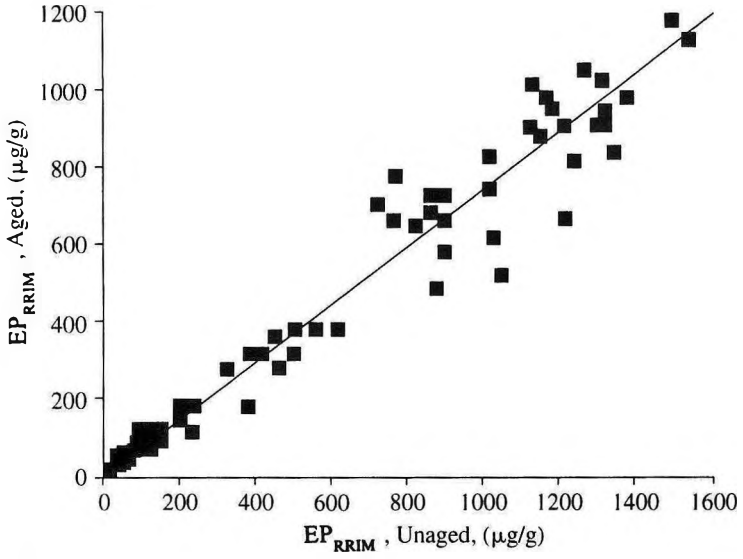

Figure 2. Relationship between aged and unaged EP_{RRIM} values for 77 lots of latex gloves. Correlation coefficient r = 0.98, P<0.001.

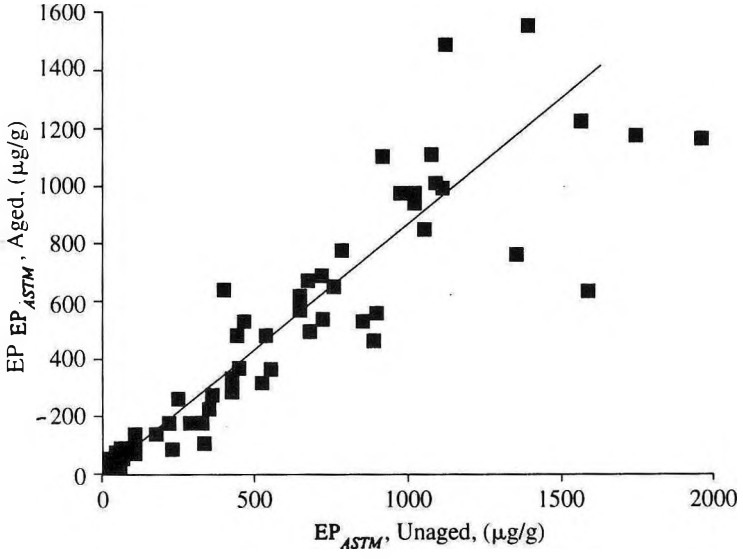

Figure 3. Relationship between aged and unaged values of EP_{ASTM} for 77 lots of latex gloves. Coefficient of correlation r = 0.92, P<0.001.

this is also the fact that the EP_{RRIM} values read higher than those of the corresponding EP_{ASTM}, for the same latex glove samples tested. Furthermore, it is noteworthy that, as shown by the present findings, low EP_{RRIM} of up to 100 μg/g corresponded to EP_{ASTM} of similar range, *i.e.* up to 107 μg/g (Table 2), while low EP_{ASTM} values of 100 μg/g and less were found to be associated with a much wider range of EP_{RRIM}, *i.e.* 267 μg/g and lower *(Table 3)*. Of special interest is the fact that gloves with EP_{ASTM} of 50 μg/g (sensitivity limit of the *ASTM* test) and less, were shown to have EP_{RRIM} varying from 206 μg/g to < 20 μg/g. This could mean that the RRIM test is capable of yielding more sensitive measurements than the *ASTM* test. On the other hand, it could also be argued that such behaviour might be due to differences in response to interference by the two tests. However, there is presently no data to substantiate this. The two sets of EP data are, in fact, very well correlated, coefficient of correlation, $r = 0.93$, $P < 0.001$ and $n = 90$.

Although both tests measure only the total extractable proteins, and not the allergens alone, the EP data so obtained could be of relevance if they relate well to the allergen contents or allergenicity of the test samples. This has, in fact, been shown to be the case for EP_{RRIM} [11,12]. Gloves with EP_{RRIM} contents varying from > 1000 μg/g to < 20 μg/g were both evaluated for their allergen levels using the IgE ELISA-inhibition test[11] , as well as tested by the skin prick test on latex hypersensitive subjects from a European population[12] . Highly significant relationships were obtained in both cases. More importantly, EP_{RRIM} contents of about 100 μg/g and lower were shown to be associated with not only very low allergen levels, but also with very little allergic response by the sensitive persons. Such findings have rendered the EP_{RRIM} measurements useful as indicators of allergic potential of latex gloves.

There are no similar studies reported on EP_{ASTM}, but according to Sussman *et al.*[13] who recently skin prick tested some latex sensitive persons in Canada with gloves of EP_{ASTM} contents up to 50 μg/g , more than 50% of the subjects responded positively. In the light of the present observations, it may not be impossible that the gloves tested included some with EP_{RRIM} levels of as high as 200 μg/g, hence contributing to the relatively high positive responses observed. To confirm this, more studies are needed.

Effect of Accelerated Ageing

The Food and Drug Administration (FDA) of the USA, in addressing the latex allergy issue, allowed a 'Low Protein Labelling Claim' for latex medical gloves[10] in May 1995. As one of the requirements relating to the claim, accelerated ageing is necessary prior to analysis of the test sample for total extractable protein content. This is in view of the fact that the EP content might increase during storage.

The present study has in fact shown that decreases in the extractable protein contents of latex gloves were detected after the ageing process. The drop in EP could likely be due to denaturation of some extractable proteins when the dry gloves were subjected to prolonged heating, leading to certain amount of insolubilisation of these proteins. Such decreases were more apparent in the case of the powdered gloves than the powder-free gloves, suggesting that some loss of powder during the ageing process might have partly contributed to this difference.

Very occasional increases in EP have also been observed. The presence of water in the not so dry test sample could be the cause. In such cases, heating during the ageing process could have facilitated further migration of the soluble proteins towards the surface of the film along side with the water, resulting in higher EP contents.

CONCLUSION

It may be concluded that both the RRIM and the *ASTM* tests are suitable for measuring total extractable proteins of latex products. Protein values by the former test are generally higher than those of the latter test, and the two sets of data are significantly correlated. However, it should be pointed out that the EP values in both cases are not absolute, being referred to arbitrary protein standards. As such, their comparison could only be deemed more precise if done in reference to a standardised method, which is currently not yet available . But in view of the good correlations between EP_{RRIM} and allergenicity/allergen content, the EP_{RRIM} may be considered to be a useful indicator for allergic potential of latex gloves, particularly for the manufacture of low protein gloves. On the other hand, more data is required in the case of EP_{ASTM}.

Accelerated ageing of latex gloves generally has no adverse effect to their extractable protein contents.

ACKNOWLEDGEMENT

The author wishes to thank the Director of RRIM for permission to present this paper. She also likes to acknowledge the very capable assistance of R. Vijalakshmi, Ng Chong Seng and Abd. Aziz Awang. Contribution by Mok Kok Lang during the initial stage of the study is much appreciated.

REFERENCES

1. *Proceedings of International Latex Conference: Sensitivity to Latex Medical Devices, (1992), November 5 – 7, Baltimore, Maryland, USA.*

2. TURJANMAA K., LAUREN K., MÄKINEN-KILJUNEN S. AND REUNALA T. (1988) Rubber Contact Urticaria: Allergenic Properties of 19 Brands of Latex Gloves. *Contact Derm.*, **19**, 362.

3. BEEZHOLD, D.H. (1993) Measurement of Latex Protein by Chemical and Immunological Methods. *Proceedings of Latex Protein Allergy: The Present Position, Amsterdam*, 25.

4. YUNGINGER, J.W., JONES, R.T., FARAWAY, A.F., KELSO, J.M., WARNER, M.A. AND HUNT, L.W. (1994) Extractable Latex Allergens and Proteins in Disposable Medical Gloves and Other Rubber Products. *J. Allergy Clin. Immunol.*, **93**, 836.

5. HAMILTON, R.G. AND ADKINSON, N.F. (1994) Serologic Assays for Antigens and Antibodies. *Immunol. Allergy Clin. N. Amer.*, **14**, 351.

6. FARIDAH YUSOF AND YEANG H.Y. (1992) Quantitation of Proteins from Natural Rubber Latex Gloves. *J. nat. Rubb. Res.*, **7(3)**, 206.

7. Test Method for the Analysis of Extractable Proteins in Natural Rubber Products (1996) *Malaysian Standard Test, MS 1392 : 96P.*

8. Standard Test Method for Analysis of Protein in Natural Rubber and its Products (1995) *ASTM Designation 5712 – 95.*

9. PALOSUO, T., MÄKINEN-KILJUNEN, S., ALENIUS, H., REUNALA, T., ESAH YIP AND TURJANMAA, K. (1997) Measurement of Natural Rubber Latex Allergen Levels in Medical Gloves by Allergen-specific IgE ELISA-inhibition, RAST-inhibition and Skin Prick Testing. Submitted for publication.

10. Interim Guidance on Protein Content Labelling Claim for Latex Medical Gloves (1995) Food and Drug Administration (FDA), Centre for Devices and Radiological Health (CDRH) and Office of Device Evaluation (ODE) Document.

11. ESAH YIP, PALOSUO, T., ALENIUS, H. AND TURJANMAA K. (1997) Correlation between Total Extractable Proteins and Allergen Levels of Natural Rubber Latex Gloves. *J. nat. Rubb. Res.*, **12(2)**, 120.

12. ESAH YIP, TURJANMAA, K., NG, K.P. AND MOK, K.L. (1995) Residual Extractable Proteins and Allergenicity of Natural Rubber Products. *Proceedings of International Conference on Latex Protein Allergy: The Latest Position, Paris*, 33.

13. SUSSMAN, G.L. AND BEEZHOLD, D.H. (1997) Safe Use of Natural Rubber Latex. *Allergy and Asthma Proc.* **17(2)**, 101.

APPENDIX 1. RRIM AND ASTM *PROTEIN TESTS: MAJOR DIFFERENCES*

No.	Procedure	RRIM Protocol	*ASTM* Protocol
1	Extraction		
	Extraction medium	PBS (0.01 M, pH 7.4)	Distilled/deionised water
	Volume/g of sample	5 ml/g	10 ml/g
	Temperature	23° ± 2°C	37° ± 2°C
	Time	3 h	2 h
2	Protein precipitation/concentration		
	Precipitants	TCA/PTA	DOC/TCA/PTA
	Final concentration of TCA	4.4%	5.5%
	PTA	0.2%	5.5%
	DOC	–	0.014%
	Resolubilisation – medium	0.2 *M* NaOH	0.1 *M* NaOH
	– volume	1 ml to 6 ml	0.25 ml/1.0 ml
	Concentration	6× – 1×	4× – 1×
	Sedimentation rate	10 000 × g/30 min	3000 × g/30 min or 6000 × g/15 min
3	Lowry microassay		
	Volume of protein solution	800 µl	200 µl
	Alkaline copper solution	300 µl (citrate)	100 µl (tartrate)
	Reaction time	10 min	0 min
	Folin reagent – strength	72% of 2N	Dilute (not specified)
	– volume	100 µl	800 µl
	Colour development	30 min	15 min – 30 min
	Calibration standard protein	BSA	Ovalbumin

TCA: Trichloroacetic acid; PTA: Phosphotungstic acid; DOC: sodium deoxycholate; PBS: Phosphate buffered saline; BSA: Bovine serum albumin

J. nat. Rubb. Res., **12(3)**, 176–185

Effluent Treatment System for RRIM Rubber Glove Manufacturing Plant†

NORDIN ABDUL KADIR BAKTI*# AND ZAID ISA*

A prototype effluent treatment system for the Rubber Research Institute of Malaysia (RRIM) rubber glove manufacturing plant was designed and constructed at a cost of about RM 360 000. The system comprising a rubber trap, a chemical flocculation unit, a primary sedimentation tank, anaerobic and aerobic fluidised beds and a secondary sedimentation tank was designed to treat 120 m^3/d effluent. The design of the prototype system was partly based on pilot-plant studies. The construction of the prototype system was completed in September 1996. It was commissioned in January 1997. This paper discusses the development of the prototype system and the comparative evaluation with the conventional activated sludge system.

The rubber glove manufacturing industry in Malaysia has expanded rapidly in recent years due to the increase in the world demand for the product. Exports earning for the product in 1995 valued at RM 2.27 billion, an increase of about 23% over the previous year[1,2]. It contributed to about 73.3% of the total earnings from exports of latex products and 58.8% of total exports of rubber goods.

The RRIM has been actively involved in the research and development to support the rubber industry in Malaysia including the rubber glove manufacturing industry. The RRIM has recently set up a rubber glove manufacturing plant with the aim of assisting rubber glove manufacturers in solving their industrial-scale problems.

Effluent from the glove manufacturing facility is treated using a treatment system comprising a rubber trap, a chemical flocculation and a biological fluidised bed system. The design, construction and commissioning of the full-scale effluent treatment plant were carried out in-house.

This paper discusses some major aspects of the development of the prototype effluent treatment plant, including the starting-up experience and the comparative evaluation with the conventional activated sludge system.

PROCESS DESIGN

The results of the laboratory and pilot plant studies[3] were used to develop the process design of the prototype effluent treatment system. Theoretical calculations[3] were applied where experimental data were unavailable. The

† Paper presented at the International Rubber Conference 1997 Malaysia, 6–9 October, Kuala Lumpur

* Rubber Research Institute of Malaysia, P.O. Box 10150, 50908 Kuala Lumpur, Malaysia

Corresponding author

process flow diagram of the effluent treatment system developed is shown in *Figure 1*.

In rubber glove manufacturing, there are two main sources of effluent, namely, latex compounding waste and leaching tank discharge. Latex compounding waste contains uncoagulated latex and chemical sludge. It is usually discharged in batches, that is, during the cleaning of latex compounding and storage tanks. Leaching tank discharge contains pollutants leached out from rubber gloves during washing.

Latex compounding effluent is treated using a flocculant to separate out latex particles from the effluent. A rubber trap is used for recovery of latex coagula (*Figure 1*). Leaching tank effluent, which does not usually contain latex particles, can be discharged directly into the holding tank, bypassing the rubber trap.

Effluent in the holding tank is pumped into several mixing tanks where it is mixed with chemical flocculants. The flocculants combine colloidal particles into larger agglomerates which can be removed by settling. Colloidal particles in rubber glove manufacturing plant effluent comprise mainly organic and heavy metals such as zinc. At present, chemical flocculation is considered indispensable for the removal of these toxic and hazardous chemicals from the effluent prior to biological treatment.

Biological treatment of the partially treated effluent involves a fluidised bed system comprising an anaerobic and aerobic fluidised bed reactors. These fluidised bed reactors contain fine sand which is fluidised by recycling effluent. The sand has an effective size of 0.1 mm and a uniformity coefficient of 2.4. Each bed contained 0.2 m of gravel (1.5 mm to 25 mm in diameter) placed at the bottom and supported by a perforated plate. The gravel bed supports the sand particles and uniformly distributes the effluent. The design of the fluidised bed system was based on work carried out by Jeris *et al.*[4,5].

The effluent from the aerobic fluidised bed is passed through a tube settler and a sand filter to remove suspended solids from the effluent.

For the process design, estimated effluent flow rate and chemical oxygen demand (COD) concentrations were based on assumptions given in *Table 1*. Thus, the estimated average effluent flow rate was 80 m^3/d and the average COD concentration in the rubber glove manufacturing plant effluent was 500 mg/L.

EFFLUENT TREATMENT AREA AND COST

Total land area occupied by the various units of the effluent treatment plant is approximately 110 m^2. Construction cost of the effluent treatment plant is listed in *Table 2*.

Construction of the effluent treatment plant started in October 1995 and completed in September 1996. The plant was commissioned in January 1997.

REGULATORY STANDARDS

The effluent treatment plant has to comply with *Standard B* of the effluent regulatory standards[6], as specified in the Third Schedule of the Environmental Quality Regulations (Sewage and Industrial Effluents) 1978. Parameters required for analysis are given in *Table 3*.

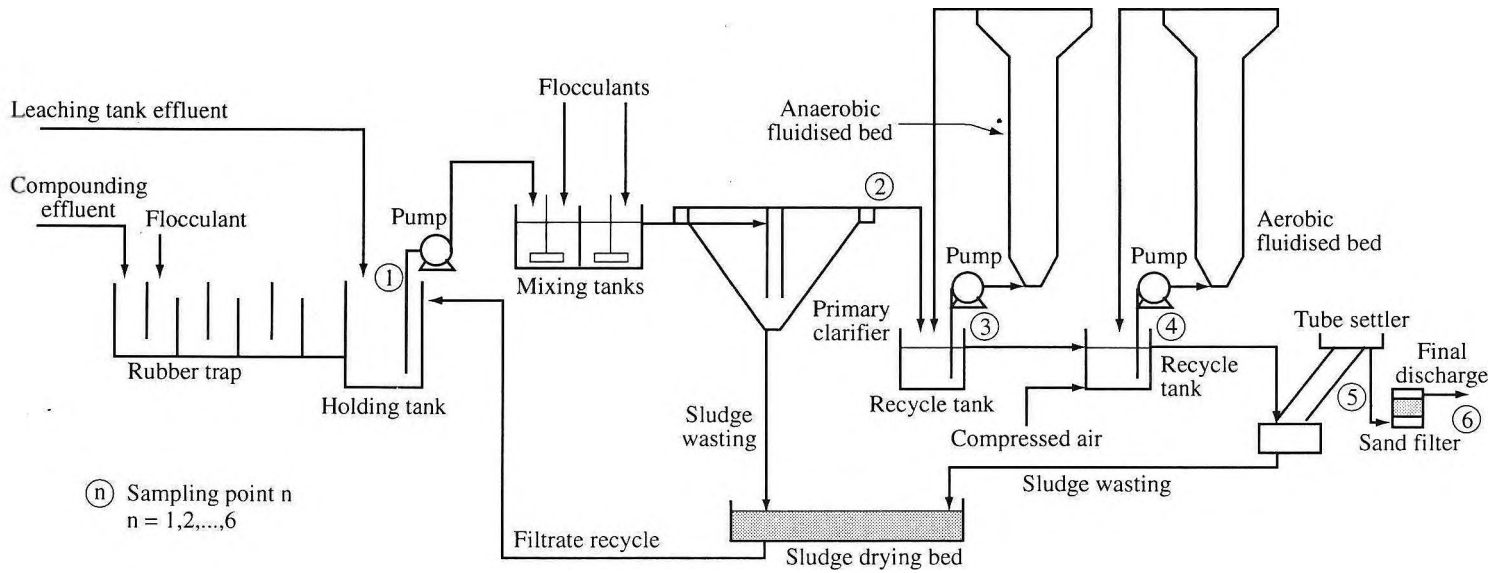

Figure 1. Schematic flow diagram of RRIM effluent treatment plant.

TABLE 1. ASSUMPTIONS[3] FOR ESTIMATING EFFLUENT FLOW RATE AND COD

Production of gloves	7 000 pieces/h/line
Production duration	24 h daily
Number of lines	2
Average COD generated per thousand pieces of glove	0.108 kg COD/10^3 pieces/d
Ratio of maximum flow to average flow	1.5
Ratio of maximum COD to average COD	1.5

TABLE 2. EFFLUENT TREATMENT PLANT COST

Item	Cost (RM)
Preliminaries, delivery, installation and miscellaneous	13 600
Civil and structural work (building, fence, gate, compound and rubber trap)	81 320
Chemical flocculation system	19 825
Neutralisation tank	4 800
Primary clarifier	14 600
Anaerobic fluidised bed reactor	32 500
Aerobic fluidised bed reactor	31 000
Air supply system	11 490
Secondary settling tank	11 500
pH controller and metering pumps	15 194
Transfer pumps	55 945
Additional structural and piping work	17 350
Professional fee for mechanical design	12 250
Electrical work	40 530
Total	361 904

EXPERIMENTAL EVALUATION

During the monitoring period (April 1997 to June 1997), the average glove production was 142 kg per week (about 18 000 pieces of glove per week). The production was less than 1% of the design production capacity. Raw materials for the glove production were prevulcanised latex, calcium nitrate (coagulant), calcium carbonate and cornstarch (slurry). Latex compounding was not carried out.

TABLE 3. REGULATORY STANDARDS

Parameter	*Standard B*
pH	5.5 – 9
BOD at 20°C (mg/L)	50
COD (mg/L)	100
Suspended solids (mg/L)	100
Lead (mg/L)	0.50
Copper (mg/L)	1.00
Zinc (mg/L)	1.00
Iron (mg/L)	5.00
Oil and grease (mg/L)	10.00

The flocculants for removing COD and heavy metals from the effluent were polyaluminum chloride (PAC) and *Magnafloc 1597*. The dosages of PAC and *Magnafloc 1597* were 50 p.p.m. and 20 p.p.m., respectively.

The average effluent flow rate was 13.8 m^3 per week (about 2.5 % of the design flow rate). The effluent discharged was let to fill the holding tank before pumping into the first mixing tank at 3 m^3/h for about 5 h weekly.

Effluent samples were taken hourly over the duration of the effluent pumping, from sampling points shown in *Figure 1*. Analyses carried out on the samples are as given in *Table 3*.

Effluent flow rates were measured using a water meter. This meter measures flow in the pipe transporting effluent from the aerobic effluent recycle tank to the tube settler.

Seeding of the fluidised beds with biological sludge was necessary for the starting-up of the fluidised beds. Each bed was seeded with about 1.25 m^3 of activated sludge. The sludge was obtained from nearby rubber factories.

Skim latex serum, with COD concentration of about 19 800 mg/L, was added periodically at a rate of about 20 L per addition into each fluidised bed to sustain growth of bacteria in the biological system. Without the addition of the serum and with insufficient effluent flowing into the system, the bacteria in the system, which require nutrients and a source of carbon for growth, will not survive. With a low population of bacteria, the fluidised beds will not be effective in treating the effluent.

In evaluating the performance of the fluidised bed system, the fluidised bed was operated as a batch reactor, that is, with no effluent flow. Effluent samples from the effluent recycle tank and the fluidised bed were taken at two-hourly intervals and analysed for COD, total and volatile suspended solids. The results of this study were compared with those obtained earlier from pilot-plant studies[3].

RESULTS AND DISCUSSION

Efficacy of Treatment System

Data collected show that the treatment plant was functioning satisfactorily although its performance at the design loading rate could not be assessed, as the effluent flow rate was below the design capacity. *Figures 2 – 4* give the results of the monitoring study.

Removals of COD, BOD and zinc from the treatment plant were 48.4%, 75% and 85.9%, respectively. Removals of the same parameters from the chemical flocculation system were 46.6%, 78.7% and 65.4%, respectively. These

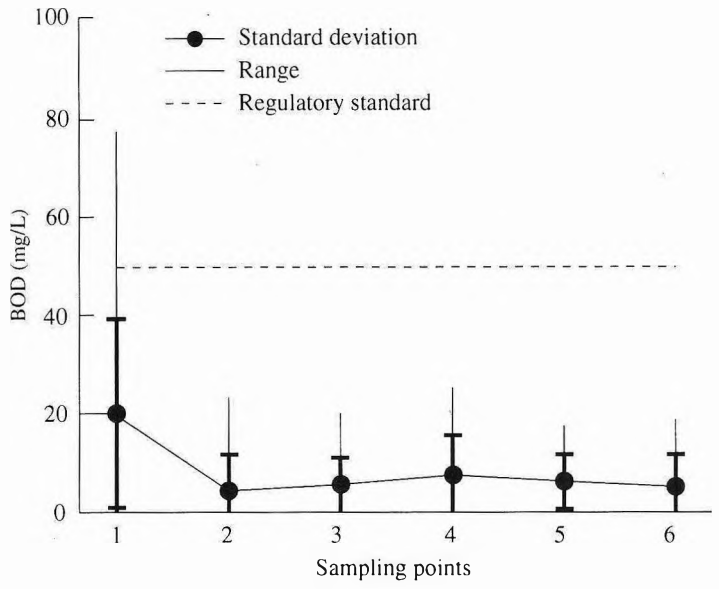

Figure 2. Effluent BOD concentrations at sampling points 1 to 6 indicated in Figure 1 *(20 samples per sampling point).*

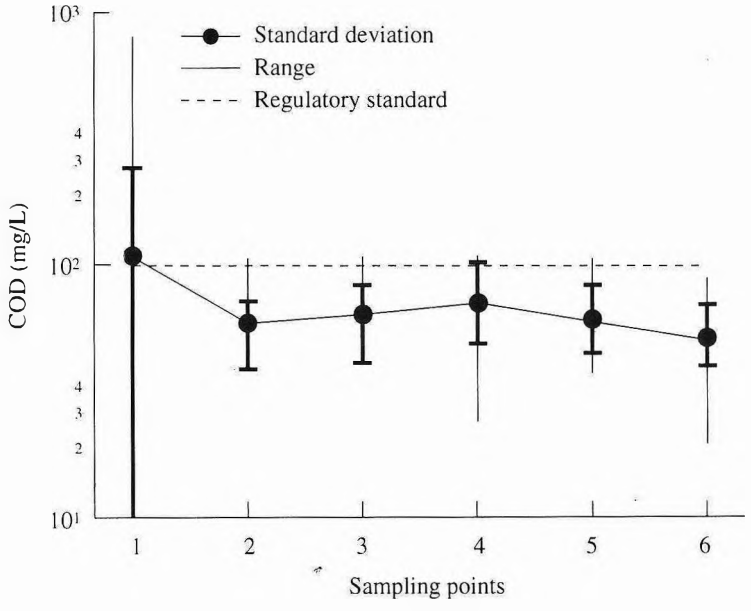

Figure 3. Effluent COD concentrations at sampling points 1 to 6 indicated in Figure 1 *(19 samples per sampling point).*

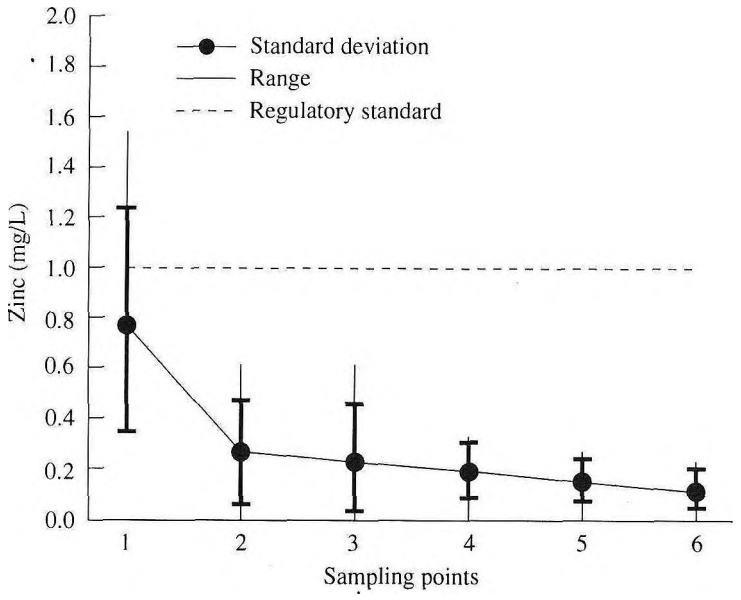

Figure 4. Effluent zinc concentrations at sampling points 1 to 6 indicated in Figure 1 *(9 samples per sampling point).*

results indicate the effluent treatment was mainly by chemical flocculation. Because the chemical flocculation system was evaluated at the effluent flow rate of 3 m^3/h (60% of the design effluent flow rate), the results are thus considered representative of its performance.

From the survey[7] of existing effluent treatment plants carried out by the RRIM, removals of COD, BOD and zinc by chemical flocculation varied from 33.1% to 48.7%, 26.7% to 43.1%, and 40.0% to 75.9%, respectively. The results obtained from the present study were comparable to those obtained from the survey.

The concentrations of COD, BOD and zinc in the untreated effluent were lower than the corresponding values obtained from the survey[7]. The average concentrations of COD, BOD and zinc in untreated rubber glove manufacturing effluent, based on the survey involving four rubber glove manufacturing factories, were 857 mg/L, 420 mg/L and 10 mg/L, respectively. The lower concentrations of COD, BOD and zinc in the untreated effluent of the RRIM rubber glove manufacturing plant were attributed to the use of prevulcanised latex for rubber glove production.

The pH of the treated effluent varied from 7.1 to 8.8, which was within the limits of the regulatory standard for the parameter. Suspended solids in the treated effluent, which varied from 8 mg/L to 35 mg/L, complied with the standard for the parameter. Oil and grease in the treated effluent, which varied from

1 mg/L to 10 mg/L, also complied with the standard for the parameter. Lead, copper and iron in the treated effluent were undetectable.

The true performance of the fluidised bed system in removing BOD could not be inferred from the data shown in *Figure 2*. Because of the already low BOD concentration (< 5 mg/L) in the effluent fed to the fluidised bed system, further BOD reduction in the fluidised bed system was not possible.

Evaluation of Fluidised Bed System

As mentioned earlier, because of the low BOD concentration in the effluent, the fluidised bed system could not be evaluated under the continuous flow conditions. As an alternative, the system was operated as a batch reactor. Skim serum was added in batches to provide the system with organic carbon and nutrients.

The reduction of COD and the biomass concentration in the anaerobic and aerobic fluidised beds were monitored at two-hourly intervals after the addition of the skim serum. From these data, substrate utilisation rates were determined (*Table 4*). The substrate utilisation rates for the full-scale units were comparable to that obtained for the pilot plant[3] operated under continuous flow conditions.

Biomass concentrations in the full-scale units were lower than that in the pilot plant (*Table 4*). These lower biomass concentrations in the full-scale system were attributed to the lower density of fine sand in the full-scale columns. The density of fine sand in the full-scale fluidised bed system was about 118 kg/m^3 and that in the pilot-scale system was about 327 kg/m^3. For the full-scale system containing sand with an effective size of 0.1 mm, the specific surface area of sand particles in the full-scale system was 1336 m^2/m^3, which was only about 45% of that in the pilot-scale reactor. The specific surface area of sand particles in the fluidised bed system used by Jeris *et al.*[5] was 3300 m^2/m^3.

The biomass concentration in the aerobic full-scale fluidised bed system was about 33% of that in the anaerobic system. This could be attributed to lower substrate concentrations in the aerobic system.

Sludge Production

Chemical sludge was produced from the chemical flocculation stage and accumulated in the primary sedimentation tank. Based on the concentration of suspended solids in the effluent from the chemical mixing tanks, the quantity of chemical sludge produced weekly was about 3.5 kg dry weight.

Biological sludge is expected from fluidised bed reactors. However, because of insufficient discharge of effluent from the glove plant, the fluidised beds were not operating at the optimum conditions and sludge accumulated in the tube settler that received effluent from the reactors was insufficient to be withdrawn.

Energy and Chemical Usage

The total power of equipment installed for the effluent treatment plant is about 21 kW. The actual energy usage was only about 2 000 kWh per month as the equipment was not operated continuously.

Chemical flocculation was carried out using 50 p.p.m. PAC and 20 p.p.m. *Magnafloc 1597*. At these dosage rates, the cost of the flocculants was RM 0.25/m^3 effluent.

TABLE 4. SUBSTRATE UTILISATION RATES IN THE FLUIDISED BED REACTORS

Fluidised bed system	SUR (kg COD/kg VSS-d)	Biomass (kg VSS/m^3)	n
Anaerobic (full-scale)	0.55 ± 0.15[a]	5.03 ± 0.35	3
Aerobic (full-scale)	1.32 ± 0.58	1.65 ± 0.19	3
Anaerobic (pilot plant)	0.49 ± 0.17	10.20 ± 2.33	4

[a]Values expressed as mean ± standard deviation
SUR: substrate utilisation rate
VSS: volatile suspended solids
n: number of runs

Biological Treatment Alternatives

Most rubber glove manufacturing factories use an activated sludge system for the biological effluent treatment. The activated sludge system is a conventional system compared to the fluidised bed system adopted by the RRIM rubber glove manufacturing plant.

Activated sludge systems use suspended growth of microorganisms and the retention time of these microorganisms in the aeration tanks is controlled by solids recycle. The performance of the system is dependent on the separation of solids in the settling tank. On the other hand, fluidised beds use biomass support particles such as sand for microbial growth and attachment. Biomass concentrations in fluidised beds are usually higher than those in activated sludge systems depending on the size of support particles. Due to the higher biomass concentrations, the overall volumetric rates of carbon conversion in fluidised beds are higher than those in the activated sludge systems. *Table 5* gives the comparison between these two systems, based on the experience of the writers.

The cost of the fluidised bed system is lower than that of the activated sludge system despite using fibre-reinforced plastic for its construction (*Table 5*). The cost of fibre-reinforced plastic is higher than that of concrete. *Table 5* also indicates that the fluidised bed system requires smaller land area.

CONCLUSION

The effluent treatment system for the RRIM rubber glove manufacturing plant was functioning satisfactorily although its performance at the design loading rate could not be assessed, as the effluent flow rate was below the design capacity.

Removals of COD, BOD and zinc from the treatment plant were 48.4%, 75% and 85.9%, respectively. The effluent treatment was mainly by chemical flocculation.

Although the BOD removal in the fluidised bed system was negligible because of low BOD concentrations in the influent, the substrate utilisation rates for the full-scale units were comparable to that obtained for the pilot-scale reactor.

TABLE 5. COMPARISON BETWEEN ACTIVATED SLUDGE AND FLUIDISED BED SYSTEM

Treatment system	HRT (h)	Volume[a] (m^3)	Surface area[b] (m^2)	Cost[c] (RM)
Activated sludge	24	120	80	90 000
Fluidised bed	1	5	20	63 500

HRT = hydraulic retention time

[a]Volume of liquid inside the tank calculated based on the HRT and the design flow rate of 120 m^3/d

[b]Surface area required by the system calculated based on the given volume, depth of 1.5 m for the activated sludge system and 5 m for the fluidised bed

[c]Construction cost of the system excluding cost of equipment and settling tank, and based on the unit cost of concrete tank of RM 750/m^3 tank volume for the activated sludge system and the unit cost of fibre-reinforced plastic of RM 12 400/m^3 tank volume for the fluidised bed

For the treatment of 120 m^3/d effluent, the fluidised bed system, compared with the conventional activated sludge system, requires lower cost and smaller land area for construction.

ACKNOWLEDGEMENT

The authors are thankful to Nor Aisah Abd. Aziz of Latex Technology Division for the information on rubber glove production and the staff of Applied Chemistry and Processing Division, in particular Wan Mohamad Wan Mukhtar for technical assistance.

REFERENCES

1. MALAYSIAN RUBBER RESEARCH AND DEVELOPMENT BOARD (1995) Consumption: Malaysia. *Malaysian Rubb. Rev.*, **16**, 2/95, 18.

2. MALAYSIAN RUBBER RESEARCH AND DEVELOPMENT BOARD (1996) Consumption: Malaysia. *Malaysian Rubb. Rev.*, **17**, 2/96, 16.

3. NORDIN AB. KADIR BAKTI (1995) Unpublished Data. Rubber Research Institute of Malaysia.

4. JERIS, J.S., OWENS, R.W. AND FLOOD, F. (1981) Secondary Treatment of Municipal Waste Water with Fluidised-bed Technology. *Biological Fluidised Bed Treatment of Water and Waste Water (Copper, P.F. and Atkinson, B. eds.)*, 112. Chichester, West Sussex: Ellis Horwood Ltd.

5. JERIS, J.S., OWENS, R.W., HICKEY, R. AND FLOOD, F. (1977) Biological Fluidised-bed Treatment for BOD and Nitrogen Removal. *J. Wat. Pollut. Control Fed.*, **49**, 816.

6. DEPARTMENT OF ENVIRONMENT (1978) Environmental Quality and Industrial Effluents Regulation 1978: Parameter Limits of Effluent of Standard A and B, P. U. (A) **12**, 64.

7. ZAID ISA AND NORDIN AB. KADIR BAKTI (1991) Unpublished Data. Rubber Research Institute of Malaysia.

J. nat. Rubb. Res., **12(3)**, 186–198

Natural versus *Synthetic Rubber Uptake in Tyres*†

KEVIN P. JONES*

In the major traditional rubber consuming areas of Europe, North America and Japan natural rubber has become a speciality rubber, in that uptake is greatest in tyres. In some countries in excess of 70% may be consumed in tyres. In economic terms this is both a considerable strength, and yet may present a considerable potential risk. Techno-economic factors which may influence the choice of elastomers in tyres and tyre products are examined. These include properties, price and availability. Factors which may influence the future health of the tyre industry, such as increasing environmental concerns, are not ignored.

Ann Gouyon[1] considers that the world natural rubber market is a paradox, because the main demand comes from the rubber processing industry, primarily the tyre sector, which according to her, accounts for 70% of the market. It is a heavy industry, with increasing capital concentrations and ever more stringent technical requirements. On the other hand over 75% of the supply comes from smallholdings, whose market share is increasing constantly, despite competition from synthetic rubber and from large estates. The latter (estates) would seem to be better placed to respond to demand from user industries, with whom they find it easier to communicate and whom they can supply with increasing quantities of controlled, consistent raw material.

At the last Meeting of the IRRDB in Sri Lanka an examination[2] was made of the displacement of natural rubber by synthetics in a wide range of products, how natural rubber had been able to regain some of these markets, and how natural rubber consumption had grown in the tyre industry due to radialisation.

The main thrust of this paper will be to examine the validity of the assertion that 70% of natural rubber is consumed by the tyre industry and to attempt to assess the vulnerability of natural rubber, especially in terms of price, within this market. Therefore, it is pertinent to begin by examining the technical strengths of natural rubber as a tyre material. These have been succinctly summarised by Baker[3] as follows:

- High green strength, tack and cohesive properties: these are essential for maintaining green tyre uniformity and stability during building and shaping operations;

- Excellent adhesion to brass-plated steel cord;

† Paper presented at the International Rubber Conference 1997 Malaysia, 6–9 October, Kuala Lumpur

* International Rubber Research and Development Board, Brickendonbury, Hertford SG13 8NP, United Kingdom

- Low hysteresis which imparts low heat generation, which in turn maintains new tyre service integrity and extends retreadability;
- Low rolling resistance with enhanced fuel economy;
- Excellent snow and ice traction for winter tyres and all-season treads; and
- High resistance to cutting, chipping and tearing.

CONCENTRATION

Figure 1 amply reinforces Ms Gouyon's concerns about capital concentration. It is clear that a handful of companies dominate tyre manufacture, and notably the 'Big Three': Bridgestone, Goodyear and Michelin. The 'Big Three' represent over half of the tyre industry in terms of turnover and a further four companies represent over 20%. Moreover, it is highly probable that these companies are leaders not only in terms of profitability and capital assets, but also dominate in terms of research, expertise and forward planning.

Nevertheless, in spite of their size these companies are not invulnerable: The Economist recently[4] questioned some aspects of the long term viability of Michelin and it is not so very long ago that Sir James Goldsmith attempted to takeover Goodyear. The next biggest group of four has shown considerable instability in the shape of the unsuccessful attempts at a merger between Continental and Pirelli. It must be assumed that stability is good from the standpoint of the supplier.

There is some vertical integration in natural rubber supply in the case of Goodyear and Michelin, especially in the case of the latter, but this is modest compared with the degree of vertical integration[5] for synthetic rubber supply, although this is not as great as might be expected. Upstream integration by the synthetic rubber industry into the petrochemical or general chemical industry, as typified by the involvement of Shell and Bayer, is probably more common than downstream integration as exemplified by the Goodyear ancillary companies which are synthetic rubber producers. Integration between the tyre and automotive industries has been rare, although Michelin had a stake in Citroën. Such an association would seem to be unlikely to develop within the current business climate where out-sourcing is being encouraged.

VALIDITY OF TYRE DOMINANCE

It is difficult to be certain whether the tyre sector does represent 70% of the market for natural rubber, as stated by Gouyon[1], although the present author[6] and his former colleagues have long assumed that this to be a feature of natural rubber consumption. Watson states that 3.1 million tonnes of natural rubber[7] are used in truck tyres (of which 2 million tonnes are used in heavy commercial vehicle tyres) as shown in *Table 1*.

According to Jankowski[8], as cited by Watson[9], only about 18% of the total rubber compound used in the tread of passenger car tyres consists of natural rubber, but the carcass and sidewalls contain 'appreciable quantities' of natural rubber. Elsewhere Watson[10] has stated that car tyres consume 1 million tonnes of natural rubber and that 500 000 tonnes are consumed in the 'other' category of agricultural, motor-cycle, aircraft tyres, *etc.* plus retreading. Furthermore, Watson argues that this leaves

TABLE 1: NR CONSUMPTION IN TRUCK TYRES

	NR	SR
LCV tyres	1.1	0.6
HCV tyres	2.0	0.5
Total	3.1	1.1

only 600 000 tonnes to be consumed by the general rubber goods industry.

To some extent these data quoted by Watson are significantly different from the interpretations made by his colleague Jumpasut[11] who indicates that take up by the tyre industry does not dominate natural rubber consumption (*Figure 2*).

Watson's data[10] imply that about 1.5 kg of natural rubber is consumed in the average passenger tyre (based on the EIU estimate of passenger tyre production in 'key countries' in 1995 of around 600 million units). A 'typical' passenger tyre probably weighs about 5 kg and this implies a total raw elastomer content of only about 2 to 2.5 kg per tyre. On this basis, Watson's estimate would appear to be excessively high. Furthermore, Watson's 'residual' 600 000 tonnes of natural rubber to be consumed within general rubber goods is excessively low. Indian statistics show that 250 000 tonnes of natural rubber are consumed in this sector. US statistics infer that at least 200 000 tonnes of natural rubber are consumed by this sector there. The other available IRSG data (for France, Germany, United Kingdom and Japan) add a further 185 000 tonnes. Thus uptake of natural rubber by the passenger tyre industry is probably nearer 500 000 tonnes worldwide rather than the 1 million tonnes suggested by Watson.

It is believed that Watson[10] overstates the demand for natural rubber in the passenger tyre sector. Clearly some is required to assist in tyre building and to provide grip on snow and ice: a market which was considered to be equal to about 30 000 tonnes per annum[6]. There is a considerable amount of activity from the synthetic rubber industry in this sector, especially from solution SBR.

Watson's 'other tyre' category is an interesting one. It includes aircraft tyres which are reputed to be manufactured mainly from natural rubber. Airliner tyres represent a very demanding application: takeoff and landing speeds are high (in excess of 300 km/h on takeoff at full load) and temperatures within the tyres can reach 150°C on landing. About 600 000 aircraft tyres of all types are produced[12] annually in the USA. Manufacture is predominantly in the hands of the 'Big Three'. This is an even more difficult sector to categorise than truck tyres. Many light aircraft are able to make use of passenger car tyres, but airliners and high performance military aircraft require specialist tyres. These latter are known to require frequent replacement, but most are subjected to multiple retreading — between six and eight times for airliners is a frequently cited figure.

The 'other' category also includes earthmover tyres, some of which weigh up to one tonne. Again this sector is supposedly dominated by natural rubber due to the high severity of service. It is believed that some industrial trucks exposed to high severity wear exploit natural rubber in their tyres. Many agricultural tyres are probably only subject to mild wear in service and are presumably manufactured mainly from synthetic rubber.

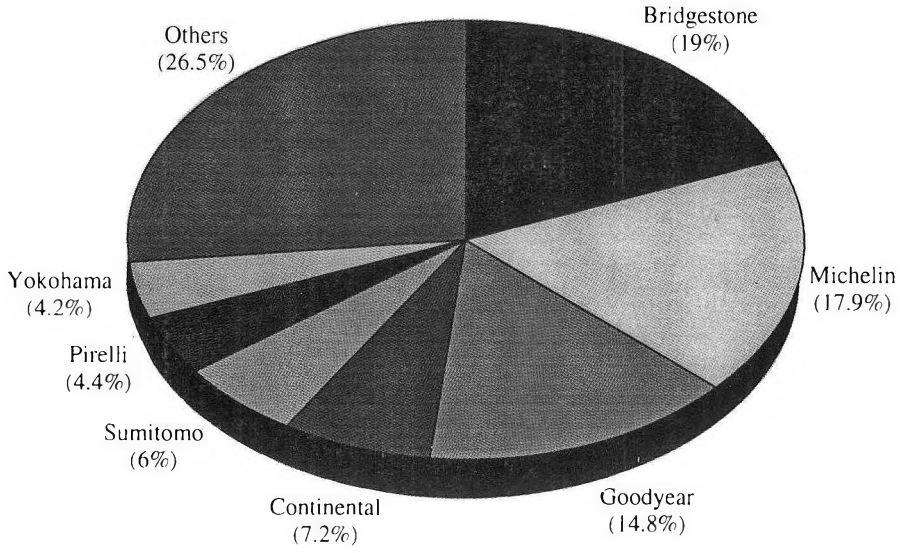

Figure 1. Market share by major companies.

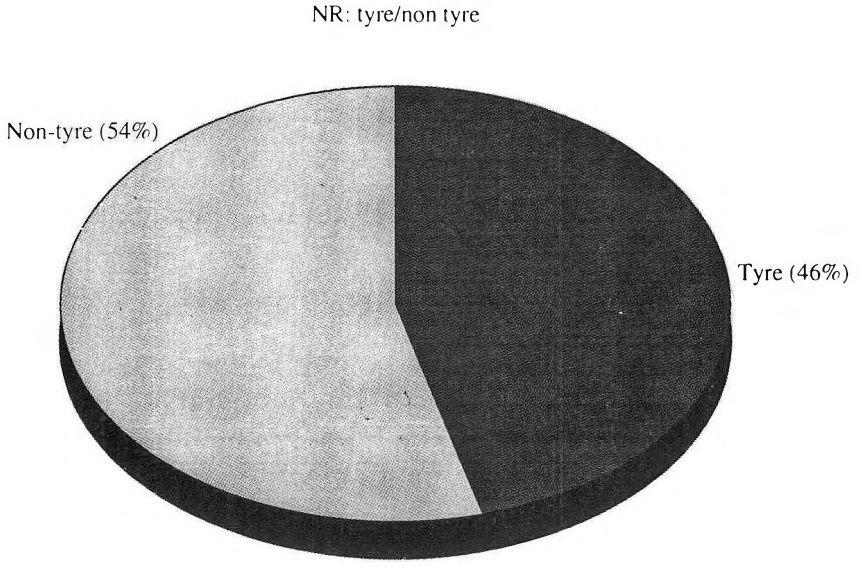

Figure 2. NR end uses (Jumpasut).

Substantial numbers of tyres are manufactured for two-wheeled vehicles. The bulk of bicycle tyres contain a minimal quantity of low grade rubber compound and sell at very low prices. Nevertheless, the new interest in mountain bikes in the United States and Western Europe has led to a new market for premium tyres and inner tubes and a new interest in the raw materials from which they are manufactured. Marketing has focused on two materials: polyurethane and natural rubber. Both tyres and tubes made from these materials (latex in the case of the inner tubes) are able to command premium prices. It is probably not without significance that some of the major tyre manufacturers (notably Continental) are taking an interest in this specialist sector, probably on the basis that most such cyclists are either car owners or are likely to become so in the near future. Motorised two-wheel vehicles are a heterogeneous group ranging from high performance motorcycles to low speed vehicles intended for cheap transport.

Examination of the relatively limited IRSG data for overall natural rubber consumption in tyres (*Figure 3*) shows that consumption in tyres as a percentage of total natural rubber consumption varies between around 50% in India to in excess of 90% in France, in excess of 85% in Japan and around 78% in the United States. In Germany about 75% of natural rubber is consumed in tyres, and until recently a similar amount was consumed in the United Kingdom, but in 1995 this surged to 84% (from 72%) in the previous year. Italian natural rubber in tyres is markedly lower, at around 65%.

It is probable in the case of the Indian and Italian data that the relatively 'low' uptake by the tyre industry infers more about the non-tyre industry than the tyre industry as such. In both cases the quantity terms are relatively high. With India this is easy to understand: India is a major natural rubber producer, but relatively minor synthetic rubber producer. Thus products which might be manufactured from synthetic rubber elsewhere continue to be made from natural rubber in India.

The Italian data have been interesting for a long time. In terms of tyre output Italy is significantly different from its neighbours (*Table 2*). Only the highly significant truck tyre data are listed, but a similar pattern is discernible from the passenger tyre production data: 29 million units were produced in Italy as against 53.5 million in France and 41.8 million in Germany. However, the amount of natural rubber consumed in the Italian non-tyre industry is also markedly higher, (36 000 tonnes as against 10 000 tonnes in France or 19 000 tonnes in the UK). The reason must merely be that natural rubber continues to enjoy market edge for some range of products manufactured in Italy which it has lost elsewhere. Knowledge of the products, and of the reasons, might be of considerable interest to natural rubber producers.

Jones and Lawson[13] observed that the tyre industry is far from homogeneous and that local factors are very important. It has long been recognised that the North American and European markets are very different. North Americans tend to travel further and, in general, expose their tyres to less stress in terms of braking and cornering. There tends to be a greater requirement for wet grip in Europe. The Japanese market for vehicle use is approaching saturation and this has a very marked effect upon vehicle design and life: there is a general tendency to restrict vehicle life by imposing stringent tests as vehicle age increases.

TABLE 2: PERCENTAGE UPTAKE IN TYRES (*VERSUS* NON-TYRE)/TRUCK TYRE PRODUCTION (MILLION UNITS)

Country	% uptake	Production
Italy	65	3.0
Germany	74	6.1
France	94	5.7
India	51	8.6
USA	79	45.0
Japan	86	44.5

For instance, the Japanese enjoy a high standard of living and are extremely skilled at designing and manufacturing cars both for a major domestic market and for export, but Japanese car ownership on a per capita basis is significantly lower than in the USA (*Table 3*). Per capita car ownership in typical West European countries lies between the two. In some countries car ownership may be less significant than total vehicle ownership and *Table 4* shows that this is so, especially in the case of China, but this *Table* is also indicative of the way in which there are more vehicles than people to drive them in the USA. The figure of 1.2 persons per vehicle is lower than the number able to drive them as allowance has to be made for children, the blind and the incapacitated. This does have a major significance for replacement tyre sales.

TABLE 3: PERSONS PER CAR

USA	1.9
France	2.3
United Kingdom	2.3
Japan	2.8
Switzerland	7.1
Korea	7.3
Malaysia	7.9
Brazil	12.5
Thailand	37.3
Indonesia	42.4
India	245
China	500

TABLE 4: PERSONS PER VEHICLE

USA	1.2
Malaysia	6.7
Brazil	10.4
Russia	10.7
Thailand	18.9
India	144.6
China	168.5

Vehicle use in Japan is also lower. Japanese cars average about 10 400 km per annum as against 17 800 km in the USA. In the case of commercial vehicles the difference is even more marked: 22 000 km in the USA as against 11 800 in Japan. The reason is that Japan is a group of mountainous islands in which space is very limited, whereas the USA is still the land of great open spaces. In Japan potential

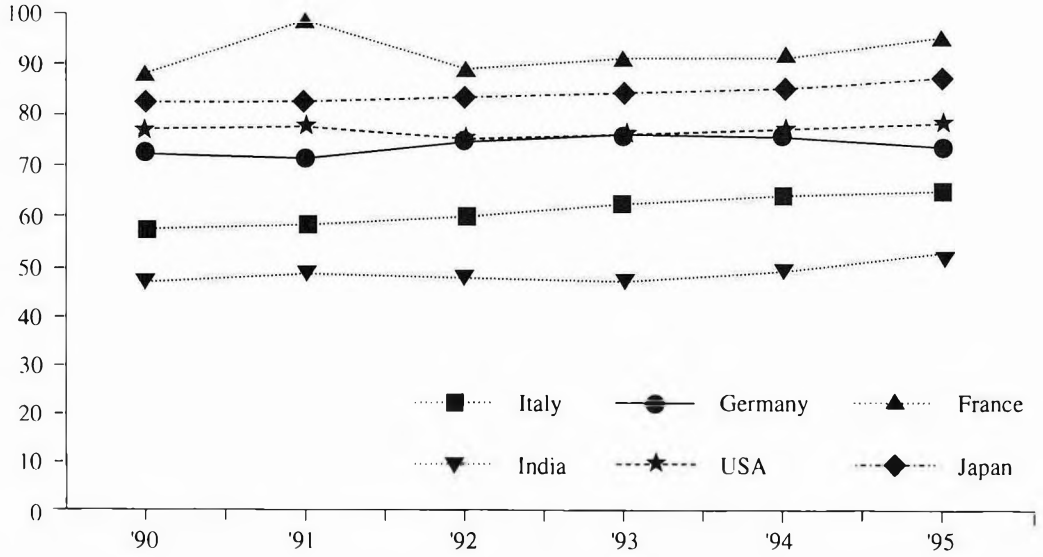

Figure 3. NR consumption in tyres as percentage of total NR consumption.

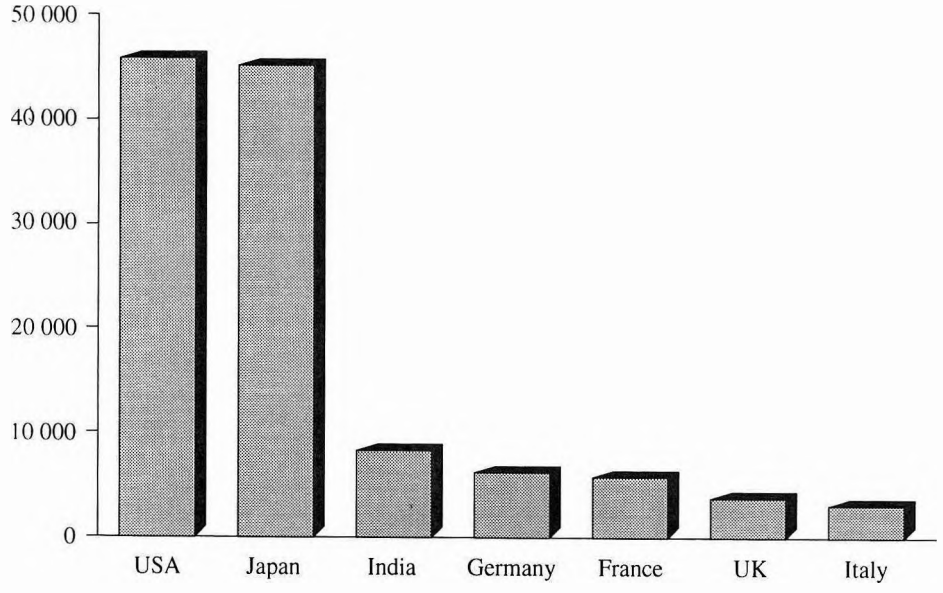

Figure 4. Truck tyre production in 1995.

car purchasers have to be able to demonstrate the availability of parking space before a transaction can take place. Parking in Tokyo can cost as much as ¥60 000 per month. Japanese cars are subject to the shaken test regime, which is intended that vehicles should have a short life as tests become progressively more demanding with vehicle age. In the USA many families have several cars.

Although the United Kingdom has a smaller motorway network of 3 000 km than Germany (11 000 km), it appears to operate relatively more trucks. As expressed in freight tonne kilometres, the Germans carry more freight by road and far more by rail and inland waterway than the British (*Table 5*). The reasons for this are complex, and partially reflect the varying definitions of commercial vehicle which tend to be based on vehicle taxation. The only certainty is that geography favours transport by both railway and internal waterway in Germany. German railways have ready access to a continental network; railways on Great Britain did not share this advantage until the Channel Tunnel opened. The enormous movement of freight by all modes in the USA is noteworthy.

Great care needs to be taken in the interpretation of statistics, especially when they relate to vehicles. Japan has a commercial vehicle park which has grown to be half that of the USA and over ten times the size of that in Germany: this is on the basis of statistical data gathered by the Society of Motor Manufacturers and Traders (SMMT). The nature of these vehicles varies greatly. In 1986, 18% of German commercial vehicle production consisted of 'large trucks' (*i.e.* with a gross weight in excess of 9 tonnes), whereas 7% of United States and only 1% of Japanese truck output was of this size. Nearly 98% of Japanese trucks in use have a gross weight of under 5 tonnes. With the exception of special vehicles, it is illegal to operate trucks in excess of 26 tonnes in Japan. Like Japanese cars, Japanese trucks do not travel far (11 000 km); British trucks are used far more intensively (about 50 000 km).

The dominance of the USA in both passenger car and truck tyre production is shown very clearly in *Figures 4* and *5*. The data relating to truck tyres for Japan calls for comment as it is highly improbable that the actual tyres being manufactured are comparable with those manufactured in either the USA or, more particularly, in Western European countries, although the US situation is complicated by the very high ownership of pick-up trucks for personal mobility rather than freight transport.

SUBSTITUTION BY SYNTHETICS

During the relatively rare periods when natural rubber prices are high there are frequent references in the trade press to firms stating that it is their intension to displace natural by synthetic should the price trend continue. The quarterly overall surveys produced by the Economist Intelligence Unit in *Rubber Trends* and the similar pronouncements by Landell Mills tend to reinforce this view of competitive volatility which paints a picture of consumers watching for changes in the relative prices of natural and synthetic. In part, such statements tend to be 'political' in that the speakers by stating something hope that it will impinge upon the future (and lead to lower prices). For instance, in mid-1994 Goodyear's Director of Rubber Purchasing, Gary Miller, stated[14]: 'The ability of supply and violent price fluctuations are worrisome for us at Goodyear... should the

TABLE 5: FREIGHT MOVEMENT: 1994: BN TONNE KILOMETRES

Country	Road	Rail	Waterway
France	122.1.	49.7	7.5
Germany	153.8	70.4	63.3
Italy	187.5	22.9	0.1
UK	140.7	14.4	0.2
Japan	275.9	25.4	–
USA	1326.0	1519.6	507.0

price rise too high, and the supply become inadequate, Goodyear will be forced to use greater quantities of synthetic rubber'. A more forceful view was expressed by Thomas Cole, President of the RMA[15]: 'The increased cost of natural rubber is driving domestic (*i.e.* US) consumers to substitute more and more synthetic rubber for natural, and consequently demand for synthetic rubber will increase while natural rubber demand decreases.'

An attempt was made[2] to substantiate these claims for switching between natural and synthetic on the basis of price. Data have been examined for the period of high natural prices during 1995 and subsequently. The data relating to France (*Figure 6*) do appear to show that the high natural rubber prices in 1995 did lead to a brief switch away from natural, but that this was followed by a recovery in uptake.

The data for Japan (*Figure 7*) may show some marginal loss in market share for natural rubber, but the picture is far from clear. The data for the USA (*Figure 8*) do not appear to produce a clear pattern for switching, although this does not match the comments made by Cole of the RMA. Expressed as a percentage, the natural rubber share of the total elastomer market in tyres varied between a low of 37.8% and a high of 39.7% within individual quarters for the three years 1994–1996. It is even possible that the buoyant railroad freight industry (*Table 5*) may have a greater influence upon natural rubber consumption in tyres than price competition from synthetics. As French uptake is dominated by one major consumer, Michelin, it is possible that action by this one corporation is more noticeable, and may have even been effective in damping price movements.

A unique situation persists in Russia where only 16 000 tonnes of natural rubber are consumed as against in excess of 400 000 tonnes of synthetic. In this case domestic long-displaced natural rubber in both tyre and non-tyre end uses. Russia has lagged behind most countries in the adoption of lead-free petrol and this has enabled it to exploit its C5 stream for isoprene production instead of producing MBTE as an additive for lead-free petroleum. It is difficult to know for how long Russian economic imperatives will be tolerated to mask its environmental problems.

CONCLUSION

The composition of tyres and the proportion of natural rubber used in tyres *versus* other uses

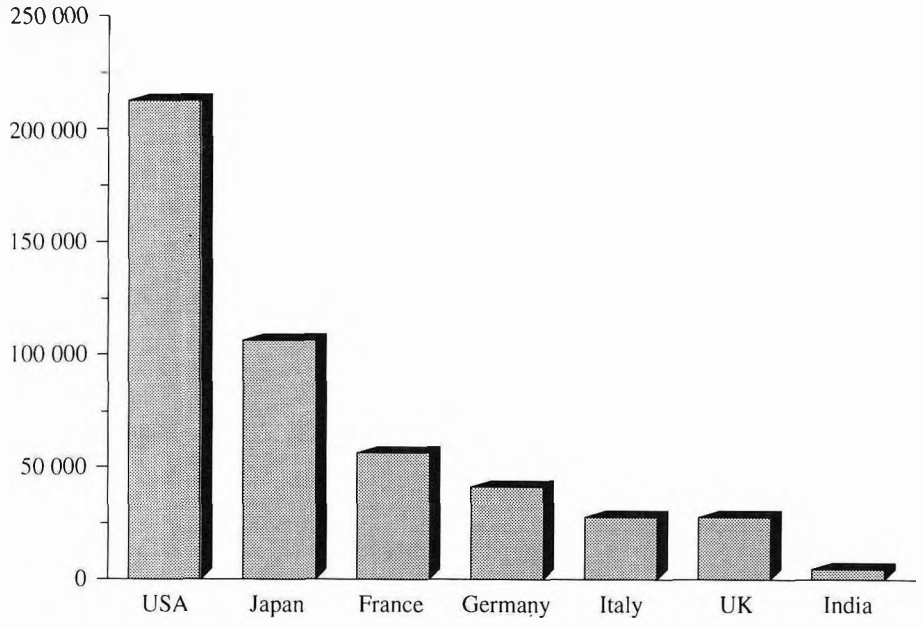

Figure 5. Car tyre production in 1995.

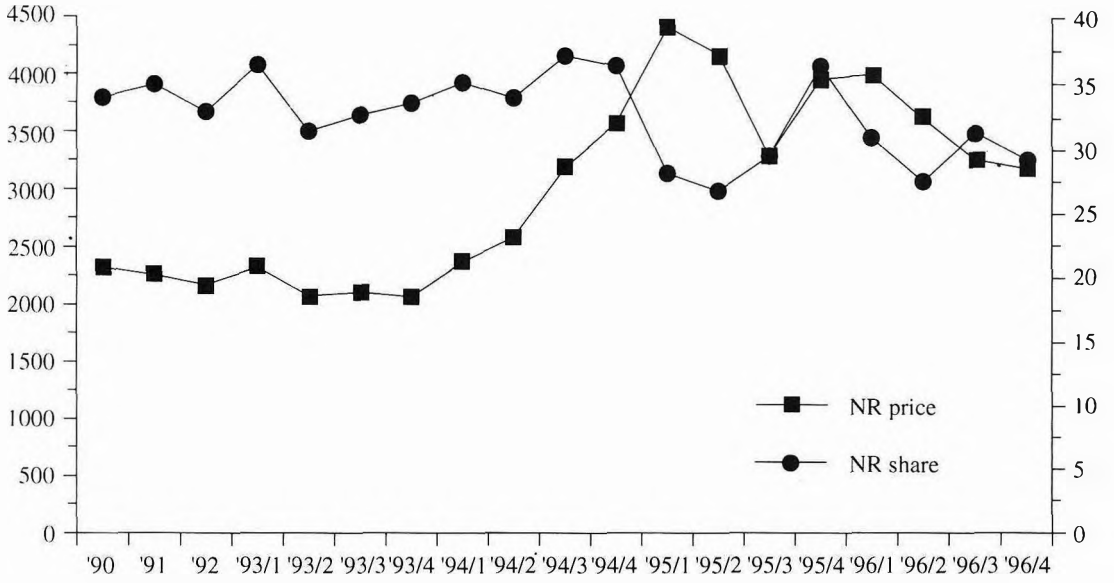

Figure 6. France: NR share of total elastomer consumption in tyres.

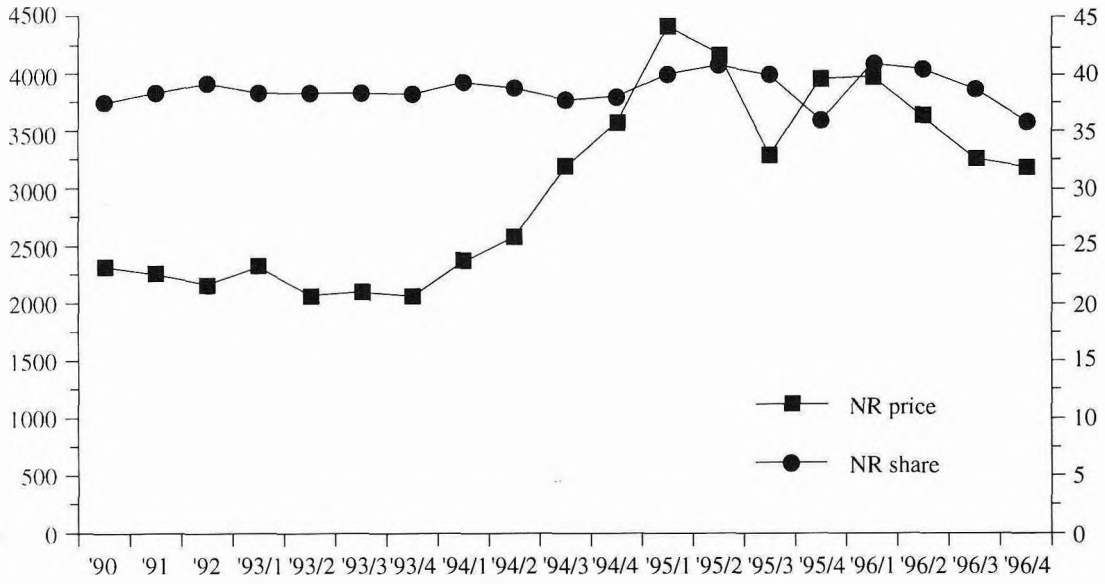

Figure 7. Japan. NR share of total elastomer consumption in tyres.

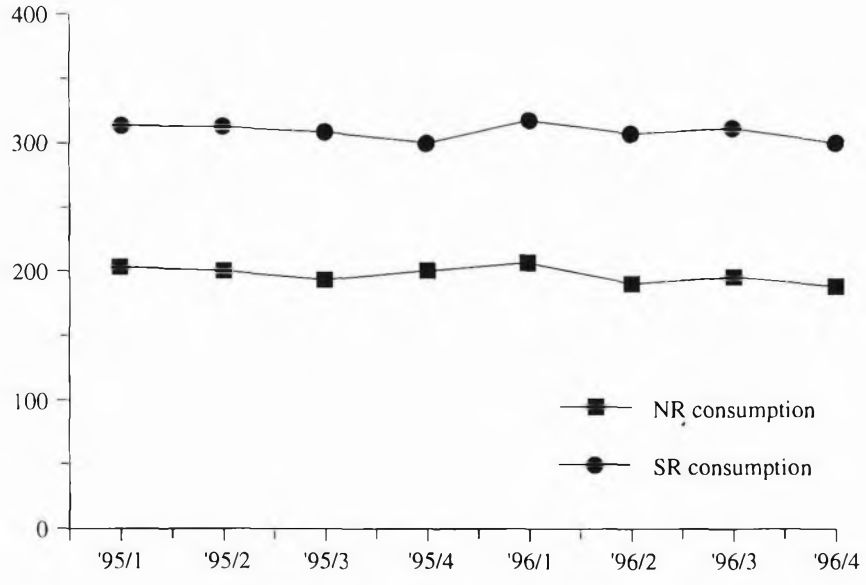

Figure 8. United States: NR share of total elastomer consumption in tyres.

are non-trivial questions. If Watson is correct in his assumptions (and it has been shown that these do appear to be completely valid) then the major market for dry natural rubber is in tyres. In theory, it should be possible to gear natural rubber production to meet the needs of the major consumer. In the past efforts have been made to do this, but these have apparently failed as the primary customer criterion appears to be one of low cost. Another, and highly positive, aspect of tyre composition is that tyres form the major scrap problem for elastomers. Nevertheless, the high level of natural rubber contained within the discarded tyres makes disposal far simpler as combustion will not significantly increase global carbon dioxide levels as the rubber trees are highly capable of reutilising the carbon dioxide released through combustion as a 'feedstock' for further latex production. This is highly significant as it is virtually the sole positive feature within any aspect of the global automotive industry apart from the ability of being able to recycle most metallic vehicle components.

Nevertheless, the competitive threat of synthetic rubber remains. Sometimes this is considered in terms of displacement when natural rubber prices are high, and there is some statistical evidence that consumers do react to displace natural rubber if there are sudden surges in price. There is less recognition that persistently low prices will damage the prospects for supply as producers switch away from natural rubber production to alternative land and labour uses.

How vulnerable is natural rubber to competition from synthetic rubber in the tyre sector? If Baker[3] and Watson[7] are correct in their assertions that natural rubber is the material of choice for truck tyres then neither the producers nor the consumers have much to fear. This is a growing market on a global scale, although the United States railroad freight statistics do demonstrate that this form of transport does still have a future provided that the economics are correct, but it is probable that the growth in demand for freight transport by road in China and Eastern Europe will provide a steady growth in this sector.

REFERENCES

1. GOUYON, A. (1996) La Production Paysanne Face au Marché Mondial du Caoutchouc. *Plantations, Recherche, DÃveloppement*, **3**, 338.

2. JONES, K.P. (1996) Substitution of Natural Rubber by Synthetic Rubber and *vice versa*. *Proceedings, IRRDB Symposium on Natural Rubber Technology and End Uses, Beruwela, Sri Lanka.*

3. BAKER, C.S.L. (1995) Latest Research and Uses of Natural Rubber. *Economic and Technical Mission for Rubber to South Africa, 14–25 May 1995.*

4. Michelin Gets a Grip. (1997) *Economist*, 1 Mar., p. 79.

5. An Anatomy of the Synthetic Rubber Industry. (1991) *Rubb. Trends, December*, p. 32.

6. BRICE, R.E. AND JONES, K.P. (1988) The Evolution of New Uses for Natural Rubber. *Natural Rubber Science and Technology* (*Roberts, A.D., ed.*) Oxford: University Press.

7. WATSON, P. (1997) Commercial Vehicle Tyres — Development and Elastomer Usage: An Update. London: IRSG.

8. JANKOWSKI, C.J. (1994) Synthetic Rubber — The Tire Industry's Critical Component. Akron: ITEC.

9. WATSON, P. (1997) High Performance Car Tyres: Their Development and Future: An Update. London: IRSG.

10. WATSON, P. (1996) Question — What are the Largest Uses of Natural Rubber? *Rubb. Dev.*, **49**, 60.

11. JUMPASUT, P. (1996) Elastomer Consumption in Tyre and Non-tyre Sectors. *Int. Rubb. Dig.*, Sept.–Dec.

12. Filling the Skies with Assurance. (1991) *Mod. Tire Dealer*, **72** (3).

13. JONES, K.P. AND LAWSON, K. (1992) Glasnost for the Rubber Industry. *Rubb. Dev.*, **45**, 3.

14. NR Prices Worry Tyre Makers. (1994) *Eur. Rubb. J.*, **176 (9)**, 3.

15. SR Consumption Increases in '95. (1996) *Rubb. Wld.*, **213 (5)**, 19.

ORDER FORM

JOURNAL OF NATURAL RUBBER RESEARCH

Please send to

The Secretary
Editorial Committee
Journal of Natural Rubber Research
Rubber Research Institute of Malaysia
P.O. Box 10150
50908 Kuala Lumpur, Malaysia

Name: .....
(Please print)

Address: .....
.....
.....
.....

No. of copies required: .....

Volume/Issue: .....
.....
.....
.....
.....

Form of remittance: Cheque/Bank Draft/Postal Order/Money Order No. .....
payable to 'Rubber Research Institute of Malaysia' (please include bank commission, if applicable). Amount: RM/US$ .....

Date: ..... Signature: .....

Journal Price

	Local	Abroad
Per issue	RM30	US$15
Per volume (4 issues)	RM100	US$50

Postage (other countries only)

	Surface mail	Airmail
Per issue	US$2	US$6
Per volume (4 issues)	US$8	US$25

JOURNAL OF NATURAL RUBBER RESEARCH

Scope

The **Journal of Natural Rubber Research** publishes results of research and authoritative reviews on all aspects of natural rubber.

Contributions are welcome on any one of the following topics: Genetics, Breeding and Selection; Tissue Culture and Vegetative Propagation; Anatomy and Physiology; Exploitation: Tapping Systems and Stimulation; Agronomic Practices and Management; Nutrition and Fertiliser Usage; Soils: Classification, Chemistry, Microbiology, Use and Management; Diseases and Pests; Economics of Cultivation, Production and Consumption and Marketing; Mechanisation; Biochemistry and Biotechnology; Chemistry and Physics of Natural Rubber; Technology of Dry Rubber and Latex; Natural Rubber Processing and Presentation, Product Manufacture, End-uses and Natural Rubber Industrialisation; Tyres; NR and SR Blends; and, Effluent Treatment and Utilisation.

The Editorial Committee, in accepting contributions for publication, accepts responsibility only for the views expressed by members of the MRRDB and its units.

Best Paper Award

Papers submitted to each volume of the **Journal** will be considered for the annual **Best Paper Award** which carries a cash prize of 1000 ringgit and a certificate. The decision of the Editorial Committee and publisher of the **Journal** on the award will be final.

Submission of Articles

General. Manuscripts should be submitted double-spaced throughout on one side only of A4 (21.0 x 29.5 cm) paper and conform to the style and format of the **Journal of Natural Rubber Research.** Contributions, to be submitted in four copies (the original and three copies) should be no longer than approximately ten printed pages (about twenty double-spaced typewritten pages). Intending contributors will be given, on request, a copy of the journal specifications for submission of papers.

Title. The title should be concise and descriptive and preferably not exceed fifteen words. Unless absolutely necessary, scientific names and formulae should be excluded in the title.

Address. The author's name, academic or professional affiliation and full address should be included on the first page. All correspondence will be only with the first author, including any on editorial decisions.

Abstract. The abstract should precede the article and in approximately 150-200 words outline briefly the objectives and main conclusions of the paper.

Introduction. The introduction should describe briefly the area of study and may give an outline of previous studies with supporting references and indicate clearly the objectives of the paper.

Materials and Methods. The materials used, the procedures followed with special reference to experimental design and analysis of data should be included.

Results. Data of significant interest should be included.

Figures. These should be submitted together with each copy of the manuscript. Line drawings (including graphs) should be in black on white drawing paper. Alternatively sharp photoprints may be provided. The lettering should be clear. Half-tone illustrations may be included. They should be submitted as clear black-and-white prints on glossy paper. The figures should be individually identified lightly in pencil on the back. All legends should be brief and typed on a separate sheet.

Tables. These should have short descriptive titles, be self-explanatory and typed on separate sheets. They should be as concise as possible and not larger than a Journal page. Values in tables should include as few digits as possible. In most cases, more than two digits after the decimal point are unnecessary. Units of measurements should be SI units. Unnecessary abbreviations should be avoided. Information given in tables should not be repeated in graphs and *vice versa.*

Discussion. The contribution of the work to the overall knowledge of the subject could be shown. Relevant conclusions should be drawn, and the potential for further work indicated where appropriate.

Acknowledgements. Appropriate acknowledgements may be included.

References. References in the text should be numbered consecutively by superscript Arabic numerals. At the end of the paper, references cited in the text should be listed as completely as possible and numbered consecutively in the order in which they appear in the text. No reference should be listed if it is not cited in the text. Abbreviations of titles of Journals should follow the **World List of Scientific Periodicals.**

Reprints. Twenty-five copies of Reprints will be given free to each author. Authors who require more reprints may obtain them at cost provided the Chairman or Secretary, Editorial Committee is informed at the time of submission of the manuscript.

Correspondence

All enquiries regarding the **Journal of Natural Rubber Research** including subscriptions to it should be addressed to the Secretary, Editorial Committee, Journal of Natural Rubber Research, Rubber Research Institute of Malaysia, P.O. Box 10150, 50908 Kuala Lumpur, or 260 Jalan Ampang, 50450 Kuala Lumpur, Malaysia.


INSTITUT PENYELIDIKAN GETAH MA
RUBBER RESEARCH INSTITUTE OF